

Published in final edited form as:

Nat Microbiol. 2021 December 01; 6(12): 1537–1548. doi:10.1038/s41564-021-00997-7.

Protective role of the Arabidopsis leaf microbiota against a bacterial pathogen

Christine M. Vogel, Daniel B. Potthoff, Martin Schäfer, Nicolò Barandun, Julia A. Vorholt*

Institute of Microbiology, ETH Zurich, 8093 Zurich, Switzerland

Abstract

The aerial parts of plants are host to taxonomically structured bacterial communities. Members of the core phyllosphere microbiota can protect *Arabidopsis thaliana* against foliar pathogens. However, whether plant protection is widespread and to what extent the modes of protection differ among phyllosphere microorganisms is not clear. Here, we present a systematic analysis of plant protection capabilities of the At-LSPHERE, which is a collection of >200 bacterial isolates from *Arabidopsis thaliana*, against the bacterial pathogen *Pseudomonas syringae* pv. tomato DC3000. In total 224 bacterial leaf isolates were individually assessed for plant protection in a gnotobiotic system. Protection against the pathogen varied with approximately 10% of leaf microbiota strains providing full protection, 10% showing intermediate levels of protection and the remaining 80% not markedly reducing disease phenotypes upon infection. The most protective strains were distributed across different taxonomic groups. Synthetic community experiments revealed additive effects of strains but also that a single strain can confer full protection in a community context. We also identify different mechanisms that contribute to plant protection. Although pattern-triggered immunity co-receptor signaling is involved in protection by a subset of strains, other strains protected in the absence of functional plant immunity receptors BAK1 and BKK1. Using a comparative genomics approach combined with mutagenesis, we reveal that direct bacteria-pathogen interactions contribute to plant protection by *Rhizobium* Leaf202. This shows that a computational approach based on the data provided can be used to identify genes of the microbiota that are important for plant protection.

Introduction

Plants do not grow as solitary organisms in nature but are host to a plethora of microorganisms, the plant microbiota¹. In particular, the bacterial microbiota has been

Users may view, print, copy, and download text and data-mine the content in such documents, for the purposes of academic research, subject always to the full Conditions of use: <https://www.springernature.com/gp/open-research/policies/accepted-manuscript-terms>

*corresponding author: jvorholt@ethz.ch.

Author contributions

CV, DBP and JAV conceived and designed the study. CV, DBP and MS performed the protection screen and validation. CV, DBP, MS and NB performed experiments testing SynComs. CV tested *in vitro* and *in planta* effect of Leaf202 and its T6SS mutant with help from MS. CV and MS extracted DNA for genome sequencing. CV analyzed sequencing data and assembled genomes. CV and DBP analyzed screening and validation data, CV analyzed SynCom data with help from MS and analyzed T6SS data. CV and JAV wrote the manuscript.

Competing Interests Statement

The authors declare no competing interests.

intensively studied across plant species, geographical locations, and years. It shows remarkable convergence at genus level and higher taxonomic rank with apparent differences among plant species at finer taxonomic resolution¹. The microbiota contributes to the plant phenotype and affects processes such as development and resistance to abiotic and biotic stresses. Plant-associated microorganisms can increase the availability of limiting nutrients²⁻⁴, influence flowering time⁵, improve resistance to drought and salinity stress⁶ and mitigate disease progression upon pathogen challenge⁷⁻¹⁰, making the plant microbiota a target of interest for agricultural applications¹¹. However, successful application of microbiome-mediated phenotypes requires an understanding of the mechanisms underlying the beneficial functions of the microbiota and how these emerge from the properties of its members, host genotypes and environmental conditions^{12, 13}.

Regarding plant protection specifically, the importance of the microbiota is evident from the addition of individual strains that lead to pathogen attenuation¹⁴. It is also apparent from suppressive soils, where the resident soil microbiota prevents pathogens from becoming established and/or causing disease^{10, 15-17}. Insights into protective mechanisms have been obtained for individual bacteria^{18, 19}. These include direct microbe-microbe interactions such as the production of antimicrobial compounds directed against the pathogen, competition for the niche (e.g. nutrient competition) or interference with pathogen virulence (e.g. via quorum quenching)²⁰. Indirect plant-mediated protection can occur via the induction of plant defence strategies as part of the innate immune system²¹. The latter enables the recognition of pathogens, as well as other microorganisms or their products via a multilayered perception system²². In addition, there is evidence that the immune system can alter the composition of the microbiota²³⁻²⁵, which in turn may also have consequence for the outcome of pathogen infection²⁶.

For the phyllosphere, the aboveground plant parts, strains of the two most common bacterial families, the *Methylobacteriaceae* and *Sphingomanadaceae*, show differences in their potential to protect the host plant against infection by the pathogen *Pseudomonas syringae* DC3000^{27, 28}. Other often detected leaf bacteria belong to the *Pseudomonadaceae* family and members of this family can have positive and negative impact on the plant host^{7, 29}. Currently, it is unclear how widespread such protective functions are in endogenous leaf-associated bacterial communities and what the implications are for leaf microbiota assembly.

Here, we systematically tested more than 200 representative bacterial leaf isolates from a publically available collection of genome-sequenced strains³⁰ for the ability to protect *A. thaliana* from infection with the foliar pathogen *Pseudomonas syringae* DC3000. Following the screening of individual strains, we examined consequences of building synthetic communities for plant protection and used genome-inferred analysis to test a mechanism of plant protection.

Results

Plant protection potential in tripartite screening experiments

To uncover how the microbiome contributes to host phenotypes, in this case plant protection, the consequences of colonization by a broad representation of individual microbiota

members was systematically assessed. We tested the potential of 224 *A. thaliana* leaf isolates, collectively referred to as the *At*-LSPHERE strain collection³⁰, for plant protection. This strain collection contains representatives of roughly 50% of the diversity observed by 16S rDNA sequencing of natural *A. thaliana* plants based on 97% OTUs³⁰. Furthermore, these strains assemble into communities resembling the natural microbiota at a phylum level in a gnotobiotic system³⁰. We used a tripartite *A. thaliana* model system and screened each of the strains *in planta* for protection against *luxCDABE*-tagged *Pseudomonas syringae* DC3000 (Pst) (see methods). Two read outs were used to monitor protection, i.e. the degree to which the pathogen was able to establish *in planta* based on luminescence emitted by the pathogen and disease scoring as established before³¹ (Fig. 1). We conducted the screening in batches, each including positive (*Sphingomonas melonis* Fr1³¹) and negative (axenic plants, mock-inoculated) controls. Some strains were included in independent experiments, which confirmed that the robustness of the assay was generally high (Supplementary Fig. 1).

Overall, the *At*-LSPHERE strains covered a range of degrees to which they conferred plant protection against Pst, from no protection to full protection, based on disease severity. Of the 224 strains tested, 18 (8%) were fully protective with most infected plants showing a phenotype reminiscent of uninfected plants and a mean protection score greater than 90 (Fig. 2, Supplementary Table 1). The majority of these strains were Proteobacteria belonging to the genera *Pseudomonas* (6), *Rhizobium* (4), *Sphingomonas* (1), *Burkholderia* (1), *Erwinia* (1), *Serratia* (1) and *Acinetobacter* (1). Other strongly protective strains were part of the phylum Actinobacteria and the genera *Arthrobacter* (2) and *Curtobacterium* (1). In addition to scoring of disease severity, we used luminescence as a proxy for pathogen proliferation³¹. Consistent with the high protection scores of these strains, luminescence values for plants inoculated with these strains prior to infection were clearly lower than for control plants, indicating that they successfully reduced pathogen colonization (Fig. 2, Supplementary Tables 1,2). Another 10 strains showed mean protection scores greater than 75. Also these strains strongly reduced disease severity and allowed most plants to survive with few disease symptoms during the time course of the experiment, but plants showed sporadic signs of disease. This is substantiated by observations at 100- and 10,000-fold higher infection titers that we tested for a subset of five strains. Strains with high protection scores were also protective at higher infection titers, while strains with protection scores of about 75 still improved protection phenotypes relative to axenic controls at high infection titers but to a lesser degree (Extended Data Fig. 1, Supplementary Table 3). Using a mean protection score cutoff of 50, in total 43 strains showed intermediate or strong protection (Supplementary Table 1). The majority of strains (179), however, did not provide protection or only marginally improved the disease phenotype of infected plants (Fig. 3a).

The protection based on the disease scoring and luminescence reduction correlated well ($R = 0.93$, $t = 36.8$, $df = 221$, $p < 2.2 \times 10^{-16}$; Extended Data Fig. 2) and high levels of pathogen colonization resulted consistently in disease symptoms (Supplementary Data File 1). However, some strains affected the phenotype of the plants by themselves or changed the resulting *Pseudomonas* disease (see Supplementary Note and Supplementary Fig. 2). Two strains (Leaf75 and Leaf50) were not scored for protection due to phenotypes that they had induced themselves and were therefore independent from Pst infection. *Serratia* Leaf50 reduced Pst colonization based on luminescence detection (Supplementary Table 2), but

showed pathogenicity by itself, even if tested with lower inoculation titer (Supplementary Fig. 2b,c). This observation is notable because all *At*-LSPHERE strains were isolated from healthy *Arabidopsis* plants grown under environmental conditions, demonstrating that individual strains are kept at bay in a natural community context.

Correlation of plant protection by *At*-LSPHERE strains to phylogeny and colonization

Next, we examined plant protection by members of the microbiota in terms of their phylogenetic distribution and plant colonization. The distribution of protective and non-protective strains within the phylogenetic tree of the *At*-LSPHERE revealed the presence of clusters of protective strains (Fig. 2). Indeed, we found a significant phylogenetic signal in the plant protection trait (Pagel's $\lambda = 0.979$, $P = 1 \times 10^{-45}$, Abouheif's $C_{\text{mean}} = 0.569$, $P = 0.001$) that was robust also to subsampling (Supplementary Fig. 3) indicating that closely related strains are more likely to have a similar protective phenotype than two randomly picked strains.

We also measured phyllosphere colonization levels of the *At*-LSPHERE strains as colony-forming units (CFU). Most strains reached densities greater than 10^4 CFU/mg, with the majority colonizing at 10^4 - 10^6 CFU/mg (Fig. 3b,c, Supplementary Tables 1,2). The highest colonization densities were found for strains belonging to the families *Enterobacteriaceae*, *Pseudomonadaceae*, *Nocardioideae* and *Microbacteriaceae* (Fig. 3d). A few strains were either not or only sporadically recovered from the phyllosphere (Supplementary Data File 1).

The integration of phyllosphere colonization capacity and protection revealed that both traits are positively correlated when all strains are considered (Pearson's correlation of $\log_{10}(\text{CFU/mg})$ and protection score, $R = 0.47$, $t = 7.97$, $df = 223$, $P = 8 \times 10^{-14}$; Spearman's $\rho = 0.49$, $P = 9.8 \times 10^{-15}$; Fig. 3c). Strains with a protection score larger than 75 were also good colonizers with colonization densities above 10^5 CFU/mg. However, the opposite was not necessarily the case. Many strains showed a high colonization capacity but were not protective. Notably, the correlation between mean colonization and mean protection score was not evenly distributed across taxa (Fig. 3d). For example, the majority of *Pseudomonas* spp. tested showed full protection, one strain (Leaf48) showed reduced protection, and one strain showed no protection (Leaf83). This difference in protection correlated with differences in colonization densities ($R = 0.98$, $t = 13.328$, $df = 7$, $P = 3 \times 10^{-6}$). Leaf83 was the only *Pseudomonas* that did not reproducibly colonize the phyllosphere of *A. thaliana* in our experimental system (Supplementary Table 2). On the contrary, for *Methylobacteriaceae* most strains colonized well with a mean of 10^5 CFU/mg, but none of the strains showed protection. For *Sphingomonadaceae* and *Rhizobiaceae*, the best colonizing strains showed some of the highest protection potential of all strains; notably however, other members of the same bacterial family did not protect.

As with plant protection, a phylogenetic signal was observed for plant colonization (Abouheif's $C_{\text{mean}} = 0.41$, $P = 0.001$, Pagel's $\lambda = 0.988$, $P = 5 \times 10^{-26}$, Supplementary Fig. 3). Thus, although both the colonization and protection phenotypes were strain specific, closely related strains tended to show similar *in planta* characteristics.

Synthetic communities tested for protection

Next, we tested combinations of strains and investigated their impact on protection. We explored randomly assembled synthetic communities (SynCom) of 10 strains (for more details on SynCom experiments see Supplementary Note). While random SynComs of strains with mean protection scores <25 did not improve protection (Extended Data Fig. 3, Supplementary Table 4), the majority of SynComs, in which strains with mean protection scores <65 were included, showed better protection than the best individual strain within the SynCom (Fig. 4a, Extended Data Fig. 4, Supplementary Table 5). Notably, two SynComs (M10.35 and M10.21) showed a protection score >85, which is a clear improvement relative to the protection conferred by the best individual strains. We thus wondered whether the better protection might be attributed to one or two strains within the SynComs. Some mixes in which we removed individual strains only partially lost protection conferred by the community. On the contrary, in SynCom M10.35, drop-out of the two most abundant strains *Rhodococcus* Leaf278 and *Curtobacterium* Leaf261, resulted in a strongly reduced protection with a protection score of 38 compared to a protection score of 92 obtained with the full SynCom (Fig. 4b, Extended Data Fig. 5, Supplementary Table 6). *Rhodococcus* Leaf278 showed reduction of luminescence but not a great improvement in plant phenotype with infected plants showing a distinct stressed and chlorotic phenotype (Supplementary Fig. 2, Fig. 4f). As *Rhodococcus* Leaf278 was the most abundant strain in the SynCom, we tested whether removal of Leaf278 by itself would also abolish the protective effect of the M10.35 mix. Indeed, the SynCom without Leaf278 showed higher Pst colonization and stronger disease than plants inoculated with the full SynCom (Fig. 4c,d,f). Plant colonization by both *Rhodococcus* Leaf278 and the SynCom M10.35 were comparable (Fig. 4e, Supplementary Table 7). Thus the improved protection of SynCom M10.35 was not due to higher overall plant colonization but rather requires at least two different strains within M10.35, one of which needs to be Leaf278. However, not every combination of strains including Leaf278 shows high protection. We tested another SynCom with and without Leaf278 (M10.48) and found no increased protection with the full SynCom protecting to the same extent as Leaf278 alone (Fig. 4b), indicating that the effect of Leaf278 is conditional. It will thus be interesting to further deduce the mechanism of interaction leading to the improved protection by Leaf278, also in light of an arsenal of natural product gene clusters present in this strain³² and related ones³³, see also²⁰.

In addition, we used smaller synthetic communities to evaluate potential synergistic effects of strains. We hypothesized that potential additive or synergistic effects could best be identified in small mixes of strains that, by themselves, show quantifiable but not strong protection. We assembled SynComs of three strains and tested these side-by-side with the individual strains for plant protection. For two of the three mixes (M3.1 and M3.3), the community improved plant protection with regard to protection score and luminescence relative to the individual strains (Extended Data Fig. 6, Supplementary Table 8, for details see Supplementary Note). The strains already individually provided an intermediate protection score, thus suggesting additive effects. Overall, this indicates that the combination of several strains can improve protection, whereas in mix M3.2, a more complex community did not lead to an improved phenotype.

Evidence for complementary mechanisms of plant protection

Protection against infection can be due to fundamentally different mechanisms. One of these mechanisms involves the plant immune system and defense reactions by the host that are triggered by certain microbiota members²¹. Bacteria are perceived by a large arsenal of dedicated receptors (for example LRR-RLKs) that are dependent on the common co-receptors BAK1 and BKK1³⁴. We tested all protecting strains of the *At*-LSPHERE collection (mean protection score >75) as well as some strains showing intermediate (mean protection score between 50 and 75) or no protection on *bak1/bkk1* plants for loss of protection. Indeed, luminescence and hence pathogen colonization was increased in 9 of the 28 protective *At*-LSPHERE strains in the *bak1/bkk1* background (Fig. 5, for other strains see Supplementary Fig. 4). Notably, *Sphingomonas* Leaf205 and *Pseudomonas* Leaf127 were compromised in plant protection in the *bak1/bkk1* background, showing higher increase in luminescence by the pathogen compared to the axenic control as well as stronger disease symptoms on *bak1/bkk1* plants (Fig. 5, Supplementary Data File 2, Supplementary Table 9,10). This compromised protection cannot be attributed to reduced plant colonization by the *At*-LSPHERE strains in the *bak1/bkk1* background (Supplementary Data File 2). For other protective strains that resulted in higher pathogen titers on *bak1/bkk1* plants, it is not clear whether the observation is solely due to increased susceptibility of *bak1/bkk1* to the pathogen per se, as the increase in luminescence was not greater than in the axenic infected control plants (Supplementary Table 9). However, they showed a clear difference when compared to strains, which did not show higher luminescence on *bak1/bkk1* infected plants. Notably, *Xanthomonas* spp. Leaf131 and Leaf148 behaved as opportunistic pathogens on *bak1/bkk1* plants and killed numerous plants even in the absence of Pst, which was not the case in wildtype plants (Supplementary Fig. 5). This is in line with recent observations that Leaf131 and Leaf148 are opportunistic pathogens on immune-compromised *rbohD* plants²⁵. Of note, six of the 18 protective strains with mean protection score >90 showed luminescence at background level of uninfected plants and thus also completely protected *bak1/bkk1* plants. At this time, it cannot be excluded that plant-independent protection mechanisms are strong enough in the best protective strains to mask any potential plant-mediated processes. Alternatively, it is also possible that plants recognize the presence of specific strains in a BAK1/BKK1-independent manner. Importantly, in none of the strains with mean protection score >75 a complete loss of protection was observed, suggesting multiple mechanisms contributing to plant protection.

Comparative genomics to identify protection traits

Next, we wondered whether the genomes of the *At*-LSPHERE strains could be used to identify genetic features associated with plant protection. As the strains are phylogenetically highly diverse, we anticipated that differences potentially related to protection would be more readily identified in genera containing both protective and non-protective strains. As proof of concept, we focused on *Rhizobium* spp. that showed a range of protection with protective, intermediate and non-protective strains in a balanced distribution in our dataset (Fig. 6a). We identified 25 clusters of orthologous genes (COGs) present in protective strains that were absent in all non-protective strains (Supplementary Table 11, Fig. 6a). Interestingly, 14 of these 25 COGs were predicted to be type VI secretion system (T6SS)

components or T6SS-associated. T6SS have previously been described to mediate bacterial interactions by *Agrobacterium* and *Pseudomonas* spp. both *in vitro* and *in planta*^{35–37}.

To test whether the presence of the T6SS was important for plant protection, we generated T6SS mutants in *Rhizobium* Leaf202 (Fig. 6b). *In vitro* assays revealed that *Rhizobium* Leaf202 inhibited Pst and that inhibition was indeed partly dependent on a functional T6SS (Fig. 6c). We then tested Leaf202 wild type as well as the *tssL* mutant for plant protection. The *tssL* mutant allowed higher Pst colonization than the wild-type indicating that indeed a functional T6SS contributes to plant protection (Fig. 6d). This was independent of colonization density as both the wild-type and *tssL* mutant colonized the phyllosphere comparably (Fig. 6e). Overall, T6SS are widely distributed in *At*-LSPHERE strains and present in more protective strains than expected based on the overall distribution (Fisher's exact test, odds ratio 3.29, $P = 9 \times 10^{-4}$) (Extended Data Fig. 7). Thus, T6SS could be one of the mechanisms contributing to plant protection *in planta* in a subset of strains.

Discussion

Plant-associated microbes are important for the host phenotype, including plant protection. Here, we screened the *At*-LSPHERE collection composed of 224 genome-sequenced strains for protection upon *P. syringae* DC3000 infection *in planta*, thus generating systematic genotype-phenotype (plant protection and colonization) correlated data. We identified 28 of 222 strains that protected *A. thaliana* against infection with Pst. The most strongly protecting strains identified belong to the phyla Proteobacteria and Actinobacteria. Only one less protective strain was identified in the phylum Firmicutes and none within Bacteroidetes. Our analysis revealed that protection against a foliar pathogen shows a weak phylogenetic signal within the *At*-LSPHERE (Fig. 2, Supplementary Fig. 3). This points to phylogenetic conservatism of the microbial trait of protection by vertical gene inheritance, and is in-line with the observation that phylogenetic trait conservation is widespread, in particular for genetically complex traits³⁸. Nonetheless, we also observed examples of strain specificity, for example in *Pseudomonas* and *Sphingomonas* spp., which is in line with earlier observations that complex *in planta* phenotypes are often strain specific^{39–42}.

Many of the protective strains are part of the core phyllosphere microbiota taxa that are reproducibly found in association with plant leaves. Albeit at a relatively low percentage of about 10%, our screening results suggest that it is likely that protective community members are present in an environmental leaf system. Because all protective strains are colonizing at high density (Fig. 3) and these strains might be more competitive compared to others, an enrichment of protective strains might occur. It will therefore be interesting to test whether protective strains are preferentially enriched in a community context and more specifically upon stress. Such observations are also relevant in the context of biocontrol phenotypes that can be dose-dependent^{43–45}. Ultimately, under environmental conditions, higher colonization density might be a requirement for protection; however, a high colonization fitness could also be selected for as the consequence of protection. This poses the more general question whether protective strains are more often associated with and/or selected for by plants. There is evidence that plants can assemble a protective community^{7, 44}, recruit beneficial microbes^{46, 47} or enrich for groups of bacteria that

are mostly beneficial^{48, 49}. Interestingly, in our SynCom experiments where we observed community-dependent protection, we note that in some of the drop-out experiments where we removed the most abundant strain, we indeed eliminated the most protective strain (Fig. 4). However, whether this observation is robust to more complex communities or whether also removal of less abundant strains affects protection needs to be tested. In addition, it will be of interest to test other pathogens to learn the extent to which strains that are protective against Pst are also protective when encountering another pathogen and a possible pathobiome⁵⁰.

The broad screening approach conducted here also allowed circumventing likely bias that emerges from *in vitro* interaction pre-screening before testing strains *in planta*⁵¹. On the contrary, the *in planta* generated phenotypes can be integrated with other data sets that have already been assembled for the *At*-LSHERE reference collection or will be in the future. The *At*-LSPHERE strain collection has previously been tested for antagonistic interactions *in vitro*³². Only two strains (*Novosphingobium* sp. Leaf2 and *Pseudomonas* sp. Leaf58) were identified to inhibit Pst under the tested *in vitro* conditions³². While *Pseudomonas* sp. Leaf58 is among the identified strains to protect *Arabidopsis thaliana* (Supplementary Table 1), *Novosphingobium* Leaf2 does not provide plant protection in our assay. This result is in-line with the notion that antibiosis observed among strains on synthetic media is a rather poor predictor of *in planta* protection^{51, 52}. This could be due to the prevalence of other mechanisms mostly underlying *in planta* protection phenotypes, but also the lack of production of the inhibitory compound at sufficient concentrations under the environmental conditions encountered on the leaf surface, to a lack of sufficient colonization density of the commensal to cover the phylloplane, and the spatial distribution of leaf strains that is known to be patchy⁵³⁻⁵⁵.

Next to direct microbe-microbe interactions such as antibiosis or competition for nutrients⁵⁶, plants can also be indirectly protected by enhanced plant resistance²¹. Of the 28 strains with a mean protection score >75, two showed a strong reduction in plant protection in the pattern-triggered immunity compromised *bak1/bkk1* plant background. Another six strains allowed higher pathogen colonization, indicating that plant immunity is important for the full extent of protection observed by these strains. Notably, none of these showed a complete loss of protection. This finding indicates that multiple mechanisms act by complementary means to confer protection. This is also supported by the observation that additive effects occur among synthetic communities composed of 10 members and 3 members as tested here, for which M10.35 and M3.1 respectively, showed superior effects than the best protecting strain (Fig. 4 and Extended Data Fig. 6). All bacterial families for which we found protective strains (Fig. 3) harbor at least one known member described to be pathogenic^{29, 50, 57} bringing up the question on the perception and potential discrimination of pathogen versus "commensal" strains in the plant microbiota. It will thus be instructive to use the data generated here to test in how far protective and non-protective strains can be discriminated via potential plant responses they elicit.

The *in planta* screen also provided a basis for genome-inferred analyses as a way to identify modes of protection. Although systematically gathered phenotypic data can be used to identify genotype-phenotype associations⁵⁸ they pose the difficulty of distinguishing

spurious phylogenetic associations from true genotype-phenotype associations⁵⁹. Here, we exemplarily focused on one bacterial family, which showed a range of protective and non-protective strains under our experimental conditions. Genome comparisons allowed the identification of an association between the T6SS and plant protection in *Rhizobium* Leaf202 (Fig. 6). T6SSs are enriched in plant-associated microbes⁶⁰ and the T6SS can also have functions beyond microbe-microbe interactions with T6SS having also been linked to symbiosis, biofilm formation and virulence^{61, 62}. Our observation extends on other reports of T6SSs involved in microbe-microbe interactions in the plant environment^{36, 63, 64}. The Leaf202 *tssL* mutant showed attenuated but no complete loss of protection, thus hinting towards several modes of protection acting in concert as highlighted already above. Thus, it will be interesting to test additional genes found exclusively in the protective vs the non-protecting *Rhizobium* spp. for their potential contribution to plant protection. Another promising bacterial family for future genome-based analyses are *Sphingomonas* spp. that were initially thought to be composed mainly of plant protective strains based on a limited selection of strains²⁷, but was shown to harbor both protective and non-protective strains in this study with the latter outnumbering the former.

In conclusion, we show that roughly 10% of the *At*-LSPHERE strain collection protect *Arabidopsis* from *P. syringae* infection in tripartite interactions, that the potential for protection is elevated in SynComs, and that different mechanisms contribute to plant protection. Some of the latter will require spatial proximity such as bacterial warfare, while others might be indirect via the plant and thus might act systemic^{21, 65}. The data presented here highlight the identification of emergent properties of microbial communities based on abilities of individual community members and help establish causal relationships of genotypes and phenotypes.

Methods

Plant growth conditions

Arabidopsis thaliana Columbia (Col-0) and *bak1-5/bkk1-1*⁶⁶ were cultivated as described before³¹. Seeds were surface-sterilized, stratified in water at 4°C for 3-4 days before placed in 24-well plates containing 1.5 ml of MS including vitamins (Duchefa) supplemented with 3% w/v sucrose and 0.55% w/v plant agar (Duchefa). Plates were sealed with parafilm and incubated in a growth chamber (Percival, CU41-L4) set to 24°C/22°C and 65% relative humidity under long-day conditions (16 h light/8 h dark) for one week prior to switching to short-day conditions (9 h light/15 h dark). Plates were shuffled 2-3 times a week. Parafilm was removed one day before infection.

Inoculation with *At*-LSPHERE strains

At-LSPHERE strains³⁰ were grown on R-2A plates (Sigma-Aldrich) supplemented with 0.5% v/v methanol (R2A+M) and incubated at room temperature (~22°C). Cell material was resuspended in 10 mM MgCl₂, adjusted to an optical density (OD₆₀₀) of 0.2 and then diluted 1:10 to an OD₆₀₀ of 0.02, corresponding to roughly 5x10⁶ to 5x10⁷ CFU/ml. Plants were inoculated at 10-11 days by distributing 4-5 small droplets of suspension (10 µl in total) to the leaves and the center of the plants. This titer was chosen based on earlier

experiments and corresponds roughly to the carrying capacity of *A. thaliana* for the positive control strain *S. melonis* Fr1 at this plant size²⁷. Axenic control plants were inoculated with 10 mM MgCl₂. Ten-fold dilution series of inoculation solutions were prepared in 10 mM MgCl₂ and spotted on R2A+M for colony-forming units (CFU) determination. When mixtures of strains were tested, SynComs were established by mixing roughly equal ratios of the different strains (*At*-LSPHERE phyllosphere colonization is robust towards an imbalance in the inoculum³⁰). Briefly, one loop (corresponding to about 1 µl) of cell material was resuspended in 1 ml 10 mM MgCl₂ for each strain individually. Equal volumes of strain suspensions were pooled, OD₆₀₀ adjusted to 0.2 and diluted to OD₆₀₀ 0.02 for inoculation. Colony-forming units of inocula as well as of unpooled suspensions were determined by dilution series spotting onto R2A+M.

Infection with *Pseudomonas syringae* DC3000 lux

Fifteen day old plants were infected with a *luxCDABE*-tagged *P. syringae* pv. tomato DC3000⁶⁷ (here designated Pst) similar as described³¹. A dense suspension of Pst was plated on King's B medium and incubated overnight at 28°C. The lawn of Pst was scraped off after incubation with 10 ml 10 mM MgCl₂ for 10 min. The OD₆₀₀ of the suspension was adjusted to 0.3 and the suspension diluted to a final OD₆₀₀ of 0.00003. Plants were infected with 15 µl of suspension by distributing small droplets on the leaves (~13 µl) and the center (~2 µl) of the plants. This corresponded to roughly 250-300 pathogen CFU per plant. Plates were kept open to dry for about 2-3 min. Wells, in which the seeds had not germinated or in which plants were growing that could not be scored for disease development (either because growing inside the agar or upside down, other odd phenotypes) were treated with 10 mM MgCl₂ instead of Pst suspension.

Plant protection assessment

Infected *A. thaliana* plants were scored for disease development and plant protection in two different ways. As a proxy for Pst colonization, luminescence images of 24-well plates were taken at 6 days post infection (dpi) using the IVIS Spectrum Imaging System (Xenogen). To detect the Pst luminescence signal but block plant phosphorescence a 500 nm emission filter was used. The total photon flux per well was deduced by integration of the signal over regions of interest drawn on the different wells in the Living Image Software v4.2. At 13 dpi the disease phenotype was scored visually on a scale of 1-5 (healthy to dead) as described³¹. Disease phenotype scoring was whenever possible performed by two researchers. For all plant experiments, we excluded individual plants prior to analysis when plant development was not according to experience (e.g. no/late germination, growth upside down, chlorosis, plant growing in agar) or when there was a problem with the treatment (e.g. contaminated, plant mistreated) as other phenotypes could not be unequivocally attributed to Pst infection. Further, plants inoculated with Leaf75 and Leaf50 could not be assessed for plant protection (see Supplementary Fig. 2 and Supplementary Note). Plants inoculated with Leaf50 died regardless of pathogen infection or mock-treatment due to *Serratia* Leaf50. Plants inoculated with *Bacillus* Leaf75 were growing in a mucus biofilm of Leaf75 growing on top of the plant medium.

Assessment of At-LSPHERE strain colonization potential

Plates containing plants inoculated with *At*-LSPHERE strains but not infected with Pst were used to determine the colonization potential of each individual strain, similarly as described²⁷. This harvesting protocol recovers strains from the epiphytic (leaf surfaces) and endophytic (inside the leaves, apoplast) compartments without distinguishing between the two²⁷. Strains were harvested from two pooled plants per plate with replicates coming from different plates. The plants were removed from the medium with sterilized forceps; and roots and cotyledons cut off. In case of occasionally observed contact of roots and leaves, these leaves were removed, too, to prevent cross-contamination from root material. The remaining aerial plant parts were placed in pre-weighted 2 ml tubes containing 1.3 ml 100 mM sodium phosphate buffer at pH 7 supplemented with 0.2% Silwet L-77 and fresh weights recorded. Tubes were shaken for 2 x 7.5 min at 25 Hz in a Qiagen Tissue Lyser II, briefly spinned down, and sonicated for 5 min in a 2210 ultrasonic cleaner (Branson Ultrasonics). Tubes were vortexed and a suspension sample removed. Ten-fold dilution series with 100 mM sodium phosphate buffer (pH 7) were spotted in duplicates onto R2A+M square plates and incubated at RT until CFUs could be determined. When colonization was below detection limit, a value just below the detection limit (0.9 CFU) was used for calculations as described before²⁶.

Screening for plant protection of individual strains

For each of the 224 *At*-LSPHERE strains, we examined 24 plants that were scored for plant protection, i.e. luminescence and disease, and used an additional 12 plants to assess strain colonization (see above). Due to the large number of strains and the number of plant replicates, we conducted the screening in batches of up to 24 strains, each including positive controls (*Sphingomonas melonis* Fr1³¹) and negative controls (axenic plants, mock-inoculated) resulting in approximately 1000 plants per batch. All strains were screened individually in at least one round of experiments. Within each experiment, inoculation treatments were given a number prior to inoculation and were randomized between 24-well plates, with 4 treatments per plate and 4 different plates per treatment to assess plant protection and 6 treatments per plate and 3 different plates per treatment to assess colonization. Strains that showed protective or intermediate phenotypes (mean protection score greater than 50) as well as a selection of non-protective strains were validated in the screening setup described above or additionally tested for plant protection on *bak1/bkk1* (see below).

Effect of plant genotype on plant protection

A subset of strains, including all strains showing plant protection in the screen, were validated on Col-0 and at the same time tested on *bak1-5/bkk1-1* plants. At least three 24-well plates were used per strain, with half of the plate seeded with wild-type and half with *bak1/bkk1*. Opposite quarters were randomly infected with Pst or treated with 10 mM MgCl₂ at time point of infection. Plant protection was assayed using both luminescence as a proxy for Pst colonization as well as disease scoring. Plants were additionally scored at 16 dpi for disease phenotypes as differences between protective treatments can become more pronounced later on in infection. For *bak1/bkk1* plants inoculated with *Xanthomonas*

spp. no disease scoring was performed because of a *Pseudomonas* infection-independent phenotype. To assess plant colonization, combinations of three strains were distributed onto plates, so each treatment was present on 6 different plates, with half of each plate seeded with *bak1/bkk1* and the other half with Col-0. Most strains were tested once for effects of *bak1/bkk1* on Pst infection.

Screening of strain mixtures for plant protection

Synthetic communities (SynComs) were tested for plant protection on Col-0 wild-type plants as described above. Two different kind of SynComs were used. Random SynComs of 10 strains were generated (random sampling without replacement) and tested in the screening setup described above to explore the community context. In addition, a SynCom of all *Methylobacterium* strains (32 strains) was tested. These SynComs were randomized among 24-well plates, with 4 treatments per plate and at least 3 plates per treatment to assess plant protection. Furthermore, we tested SynComs of three strains that were mildly protective in the screening. The SynComs of three strains were tested together with each of the strains individually, with all four treatments combined together on 24-well plates, with at least 3 replicate 24-well plates per experiment. Selected SynComs that showed protection as assayed based on disease score and luminescence measurements were retested and uninfected plants harvested to record overall colonization densities. For a subset of SynComs, 50-100 μ l of selected dilutions were additionally plated on round petridishes to identify the most abundant strain in the SynCom.

Computational methods

A phylogenetic tree of all *At*-LSPHERE isolates as well as *Sphingomonas melonis* Fr1 was prepared using ezTree⁶⁸. RefSeq assemblies were downloaded from NCBI for all published genomes (see Supplementary Table 12). For the remaining *At*-LSPHERE strains, we cultured the strains on R2A+M agar or in R2A+M liquid medium and isolated genomic DNA using the EpiCentre MasterPure DNA purification kit according to the manufacturer's recommendations. DNA libraries were prepared using the Illumina TruSeq DNA Nano kit and sequenced on the Illumina HiSeq4000 platform (2 x 150 bp) or on the Illumina HiSeq2000 platform (2 x 250 bp). Sequencing reads were quality filtered and trimmed using the BBTools suite (v37.56)⁶⁹ and quality of reads was assessed using FastQC (v0.11.5)⁷⁰. Draft genomes were assembled with SPAdes 3.11⁷¹ and annotated with prokka (v1.12)⁷².

Average nucleotide identities were calculated using FastANI⁷³ for members of the same family/order (Supplementary Table 13).

The presence of phylogenetic signal in the plant protection against *P. syringae* and in plant colonization was tested by calculating Pagel's λ using the function `phylosig` of the package `phytools`⁷⁴ and by calculating Abouheif's C_{mean} using the function `abouheif.moran` of the `adephylo` package⁷⁵. To test whether the uneven taxonomic distribution effect the outcome and conclusion of this analysis, we additionally calculated the metrics on randomly subsampled strains (Supplementary Fig. 3). In one set of analyses, we randomly subsampled all families with more than 9 isolates. In another set, we first randomly picked one

strain from clusters with more than 99.9% average nucleotide identity and then randomly subsampled all families with more than 9 isolates. We performed 1000 iterations for each.

To identify genes potentially associated with protection in *Rhizobium* spp. a list of all assigned COGs for the publicly available genomes of *Rhizobium* spp. of the *At*-LSPHERE collection was downloaded from IMG/MER^{76, 77}. Subsequently, the list was filtered by COGs present in protective strains but not in non-protective strains. To detect the presence of type 6 secretion systems (T6SS) in other *At*-LSPHERE genomes, we looked for the presence of orthologues of the T6SS after annotating the proteins using the eggNOG-mapper⁷⁸ and eggNOG database v4.5⁷⁹. We called the presence of a T6SS if the presence of a T6SS system was either predicted by TxSScan⁸⁰ or if there were more than five of the core T6SS-associated orthologues present in the genome (COG0542, COG3157, COG3455, COG3501, COG3516-3523)⁸¹.

Generation of T6SS mutants

We targeted the structural gene *tssL* as an essential gene for T6SS in *Agrobacterium tumefaciens*⁸². Mutants of the *tssL* gene were generated in *Rhizobium* spp. Leaf202 by gene replacement with a kanamycin resistance cassette according to Ledermann et al.⁸³. DNA regions up- and down-stream of the *tssL* genes were amplified from genomic DNA and cloned using the SpeI restriction site into pREDSIX to obtain plasmid pREDSIX_HR1/2⁸³. The kanamycin resistance cassette (KmR) was cut out of pRGD_KmR with SpeI and gel-purified. The KmR fragment was then ligated into the linearized pREDSIX_HR1/2 and transformed into *E. coli* DH5 α . Transformants were selected on kanamycin and the orientation of the kanamycin cassette was identified by colony PCR. The confirmed mutagenesis constructs were transformed into *Rhizobium* spp. by electroporation. Single colonies of *Rhizobium* spp. were inoculated into half-strength LB-Lennox liquid medium and incubated at 28°C overnight. Cultures were placed on ice for 15 min and then washed 3 times with ice-cold water, followed by one wash step with ice-cold 10% glycerol and concentrated 100-fold in 10% glycerol. Aliquots (50 μ l) of electrocompetent cells were mixed with around 500 ng of purified mutagenesis plasmid and electroporated at 2.2 kV. Immediately after the pulse, 1 ml of 1/2 LB-Lennox was added and cells were regenerated at 28°C with agitation for 4-5 h. Transformants were selected on 1/2 LB-Lennox supplemented with 50 μ g/ml kanamycin and tested for double homologous recombination by PCR. Confirmed mutants (*tssL::Km^F* or *tssL::Km^R*) were restreaked at least 3 times before storing at -80°C. A list of primers used is available in Supplementary Table 14.

T6SS assay in vitro

T6SS *in vitro* sensitivity was tested using a protocol adapted from previous publications^{35, 60, 84}. Attacker (triplicate) and target strains were grown in liquid culture at 28°C in 1/2 LB-Lennox (attacker) and LB-Lennox (target) with appropriate antibiotics, respectively. Cells were pelleted, washed once and resuspended in LB-Lennox. The optical densities at 600 nm were adjusted to 0.3 (attacker) and 0.01 (target). Suspensions were mixed at 1:1 ratio and 5 μ l spotted onto LB-Lennox or R2A+M agar. After 17-24 h of incubation at 28°C, agar plugs containing the spots were placed in buffer (10 mM MgCl₂ or 100 mM phosphate buffer pH 7), vortexed for 6 min and dilution series spotted onto

R2A+M and selective R2A+M for determination of attacker and target CFU (R2A+M supplemented with 25 µg/ml rifampicin). The experiment was performed three times with similar outcomes.

Testing of T6SS dependency for plant protection

Leaf202 and its T6SS mutant (Leaf202 *tssL::KmF*) were tested in the 24-well plate system described above for plant protection with minor modifications. The Leaf202 inocula were prepared from liquid cultures grown in ½ LB-Lennox and supplemented with kanamycin when appropriate. Well-grown overnight cultures (OD > 1) were pelleted at RT, washed once with 10 mM MgCl₂, and resuspended in 10 mM MgCl₂. The optical density at 600 nm was adjusted to 0.2 and further diluted to 0.02. Plants were inoculated and infected as described above, with one half of the plate inoculated with the wildtype and the other with the T6SS mutant. Four independent plates were prepared per experiment. Two axenic control plates were inoculated with 10 mM MgCl₂ before infection. At 7 days post infection, 18 plants per condition were harvested from three plates. The experiment was performed twice with similar results.

Statistics

Data was analyzed in RStudio⁷³ with R⁷⁴ 3.6.3. No statistical methods were used to predetermine sample size. Sample size for protection assays was chosen based on previous experience³¹ and ensuring that each condition was within each experiment present on at least 3 independent 24-well plates. The disease phenotype scores were used to calculate the disease severity index (DSI) and the protection scores. The DSI reflects the occurrence of disease relative to the maximal possible disease outcome with all plants scored as dead (DSI of 100%) or all plants scored as completely healthy (DSI of 0%). The protection score of each strain was then deduced by comparing the difference in DSI between treatment and axenic controls with a protection score of 100 corresponding to all plants completely healthy and a protection score of 0 corresponding to no improvement relative to axenic controls. When several subsets of experiments were performed in parallel, values for axenic controls were combined to decrease the effect of single plants on the scaling. Luminescence data and data based on bacterial CFU counts was log₁₀-transformed prior to analysis. Data distribution was then assumed to be normal but this was not formally tested. For luminescence, log₁₀-transformed values were tested for differences relative to the axenic control by two-sided Welch's t-tests and corrected over all experiments for multiple testing using Holm's method. To compare all strains, the estimated log₁₀-transformed luminescence values were scaled relative to the values for axenic and Fr1-inoculated controls of the same experiment. The arbitrary scale was adjusted so that 100 reflected a 1.3x stronger luminescence reduction than the positive control Fr1 and 0 no luminescence reduction relative to the axenic control. To identify the effect of plant genotype on protection by individual strains, we first performed three one-sided Welch's t-tests per inoculation treatment, testing whether log₁₀-transformed luminescence values were significantly higher in infected plants relative to non-infected control plants in each plant genotype (i.e. Pst_Col-0 vs CTL_Col-0 and Pst_ *bak1/bkk1* vs CTL_ *bak1/bkk1*) and testing whether they were higher in infected *bak1/bkk1* plants relative to Col-0 plants (i.e. Pst_ *bak1/bkk1* vs Pst_Col-0). P-values were corrected using Benjamini-Hochberg's

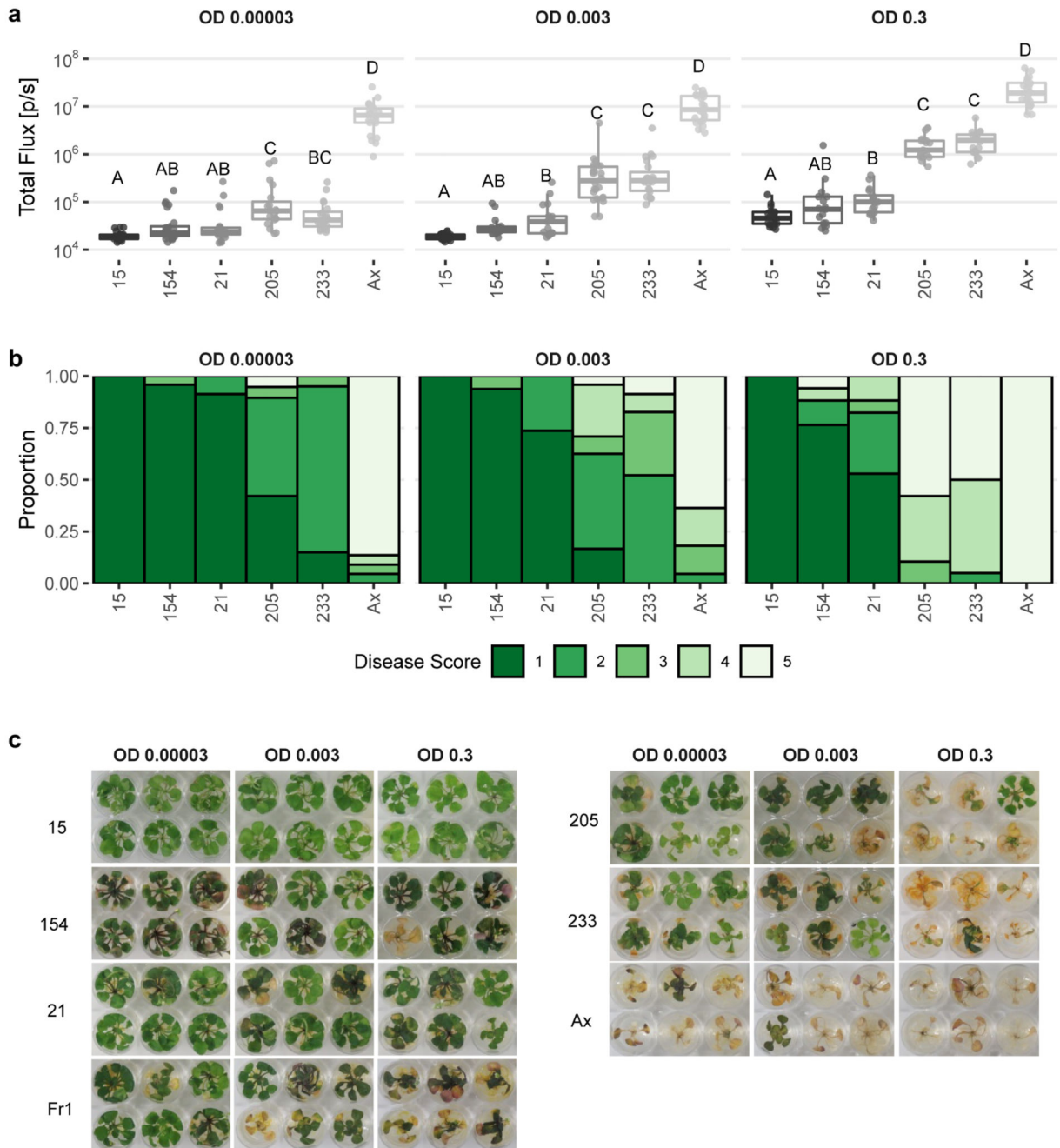
method. Furthermore, a linear model of infected log₁₀-transformed luminescence values was fitted for each strain in combination with the respective axenic control treatments. We used the full interaction model of strain treatment and genotype using experiment as a blocking factor when appropriate. When data was heteroscedastic (based on Levene's test in the R package `rstatix`⁸⁵), a generalized least squares model was fitted using the function `gl`s within the R package `nlme`⁸⁶ with `weights = varPower`. P-values of the obtained Strain:Genotypebak1bkk1 interaction estimates were corrected for multiple testing using Benjamini-Hochberg's method. For mixes of three strains, a one-way ANOVA followed by Tukey's post-hoc test implemented in the R package `emmeans`⁸⁷ was performed for each mix and experiment individually, including plate information as a blocking factor. Overall results were obtained by averaging the results from all individual experiments per treatment.

Packages used within R: `ape` (5.4-1)⁸⁸, `adephylo` (1.1-11)⁷⁵, `phytools` (0.7-47)⁷⁴, `emmeans` (1.6.1)⁸⁷, `rstatix` (0.6.0)⁸⁵, `circlize` (0.4.10)⁸⁹, `nlme` (3.1-144)⁸⁶, `ggpubr` (0.3.0), `readxl` (1.3.1), `rlang` (0.4.6), `tidyverse` (1.3.0)⁹⁰, `RColorBrewer` (1.1-2), `gridExtra` (2.3), `ggforce` (0.3.2), `scales` (1.1.1), `broom` (0.7.3)

Reporting Summary

Further information on research design is available in the Nature Research Reporting Summary linked to this article.

Extended Data

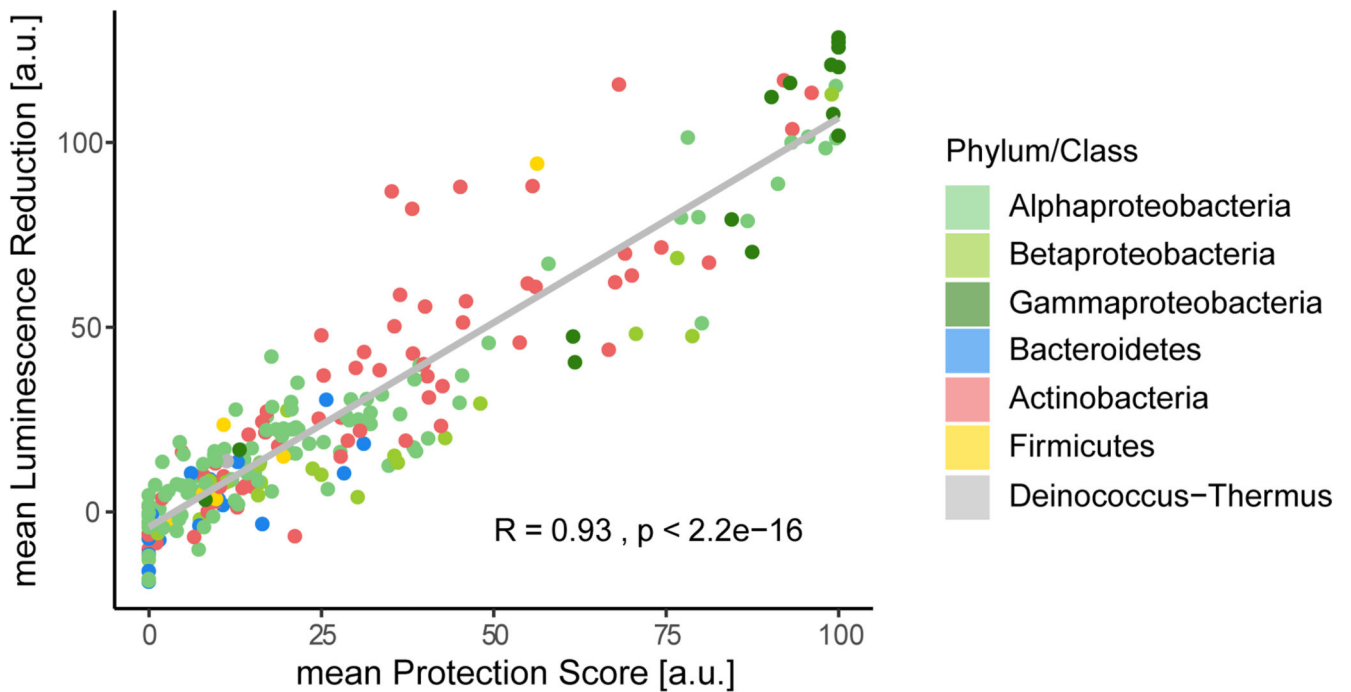


Extended Data Figure 1. Protection potential by protective *Ai*-LSPHERE strains scales with infection titer.

A. thaliana were inoculated with fully protective strains Leaf15, Leaf154 or Leaf21 (protection score >90), or with protective strains Leaf205 or Leaf233 (protection score > 75) and infected with lux-tagged *Pseudomonas syringae* DC3000 (Pst) at the regular infection titer (OD 0.00003), a 100x higher (OD 0.003) or a 10'000x higher (OD 0.3) infection titer.

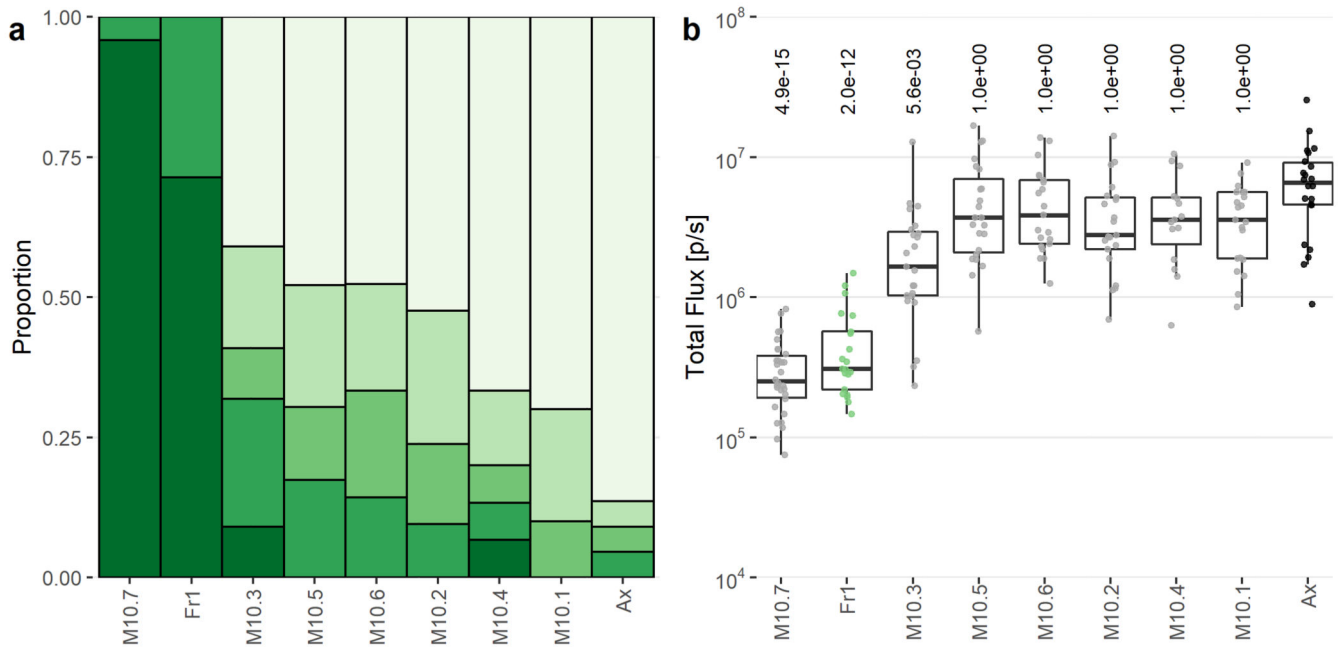
a) Luminescence indicative of pathogen colonization was measured at 6 days post infection

(dpi). Shown are boxplots and individual data points. Letters indicate significant differences for each infection titer based on ANOVA followed by Tukey's post-hoc test ($p < 0.05$, $n = 16-24$). Exact p -values and number of biological replicates are provided in Supplementary Table 3. Boxplots depict the median and interquartile range with whiskers extending to maximum 1.5x the interquartile range. **b)** Plants were scored for disease at 21 dpi on a scale of 1 (healthy) to 5 (dead). **c)** Exemplary images of plants at 21 dpi showing protection of plants by fully protective strains at high infection titers and reduced protection by Leaf205 and Leaf233 at increasing infection titers.



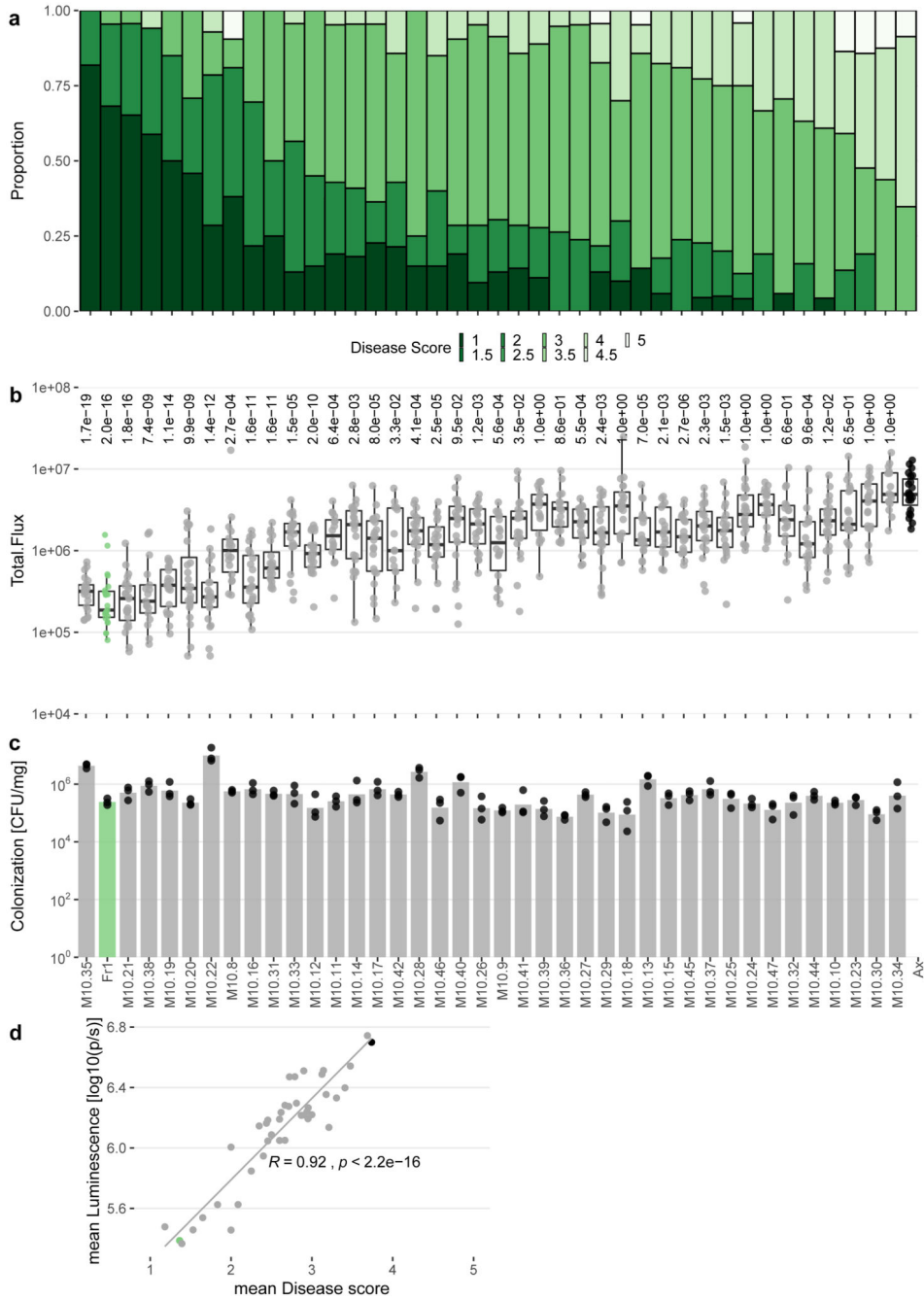
Extended Data Figure 2. Protection and luminescence reduction correlate.

Mean protection score and mean luminescence reduction (i.e. pathogen colonization reduction) correlate well for most strains (Pearson's $R = 0.927$, $t = 36.8$, $df = 221$, $p < 2.2 \times 10^{-16}$). Colors refer to phylum/class.



Extended Data Figure 3. Random SynComs of 10 non-protective strains or all *Methylobacterium* do not protect *Arabidopsis* against *Pst*.

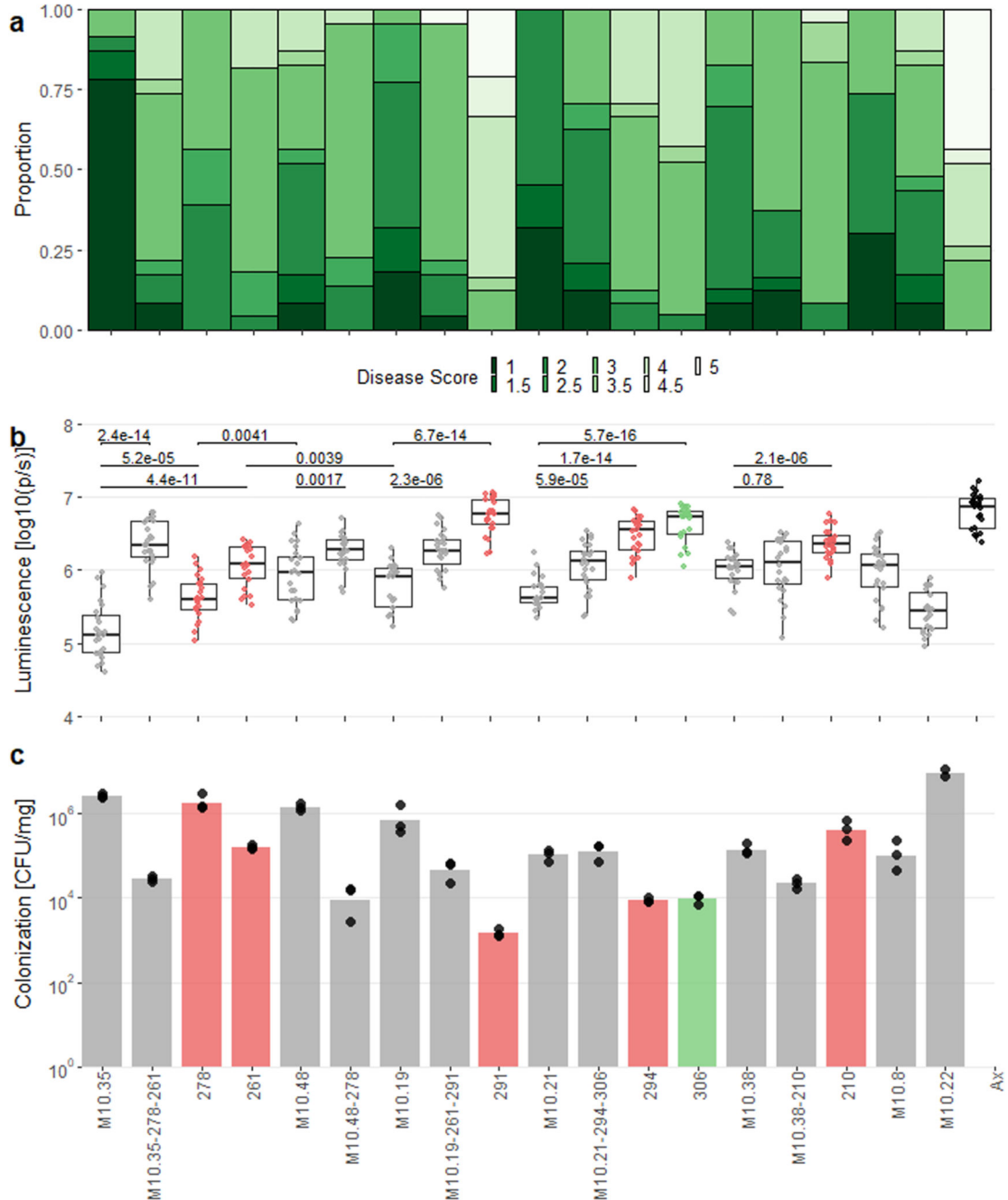
Plants were inoculated with random SynComs of 10 strains (M10.2-M10.6) containing only non-protective strains, all 32 non-protective *Methylobacterium* spp. (M10.1), Fr1 or the control SynCom M10.7, which contains one protective strain and infected with lux-tagged *Pseudomonas syringae* DC3000 (*Pst*). **a**) Distribution of disease scores on a scale from 1 (healthy) to 5 (dead) at 21 days post infection (dpi). **b**) Luminescence of the pathogen at 6 dpi. Boxplots depict the median and interquartile range with whiskers extending to maximum 1.5x the interquartile range. Asterisks in the luminescence panel indicate significant differences to axenic infected controls (two-sided Welch's t-test, corrected for multiple testing using Holm's method, $n = 15-23$). Exact p-values and number of replicates are provided in Supplementary Table 4.



Extended Data Figure 4. Random SynComs of a mixture of 10 non-protective and intermediate protective strains improve plant phenotype.

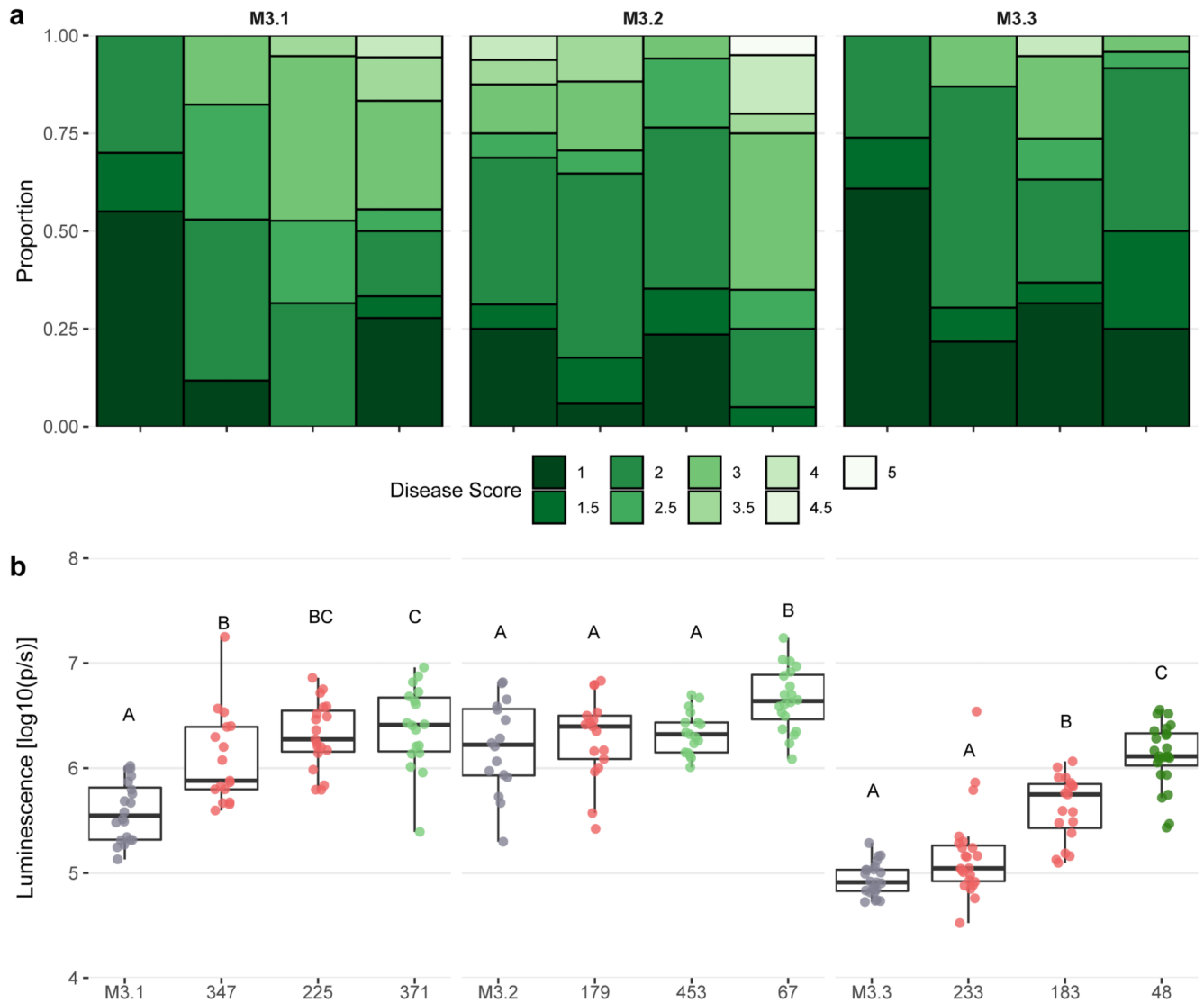
Plants were inoculated with random SynComs of 10 strains or Fr1 and infected with lux-tagged *Pseudomonas syringae* DC3000 (Pst). **a**) Distribution of disease scores at 13 days post infection (dpi) on a scale of 1 (healthy) to 5 (dead). **b**) Luminescence as proxy of pathogen colonization at 6 dpi. Boxplots depict the median and interquartile range with whiskers extending to maximum 1.5x the interquartile range. Asterisks indicate significantly different luminescence relative to axenic infected controls (two-sided Welch's

t-test, corrected for multiple testing using Holm's method, $n = 14-24$). Exact p-values and number of replicates are provided in Supplementary Table 5. **c**) Colonization by individual SynComs on non-infected plants at 12 days post inoculation. Shown are the mean and individual data points of 3 replicates consisting of two plants each. **d**) Correlation of mean luminescence and mean disease score ($R = 0.92$, $t = 14.76$, $df = 39$, $p < 2.2 \times 10^{-16}$).



Extended Data Figure 5. Drop-out of one or two strains from a random SynCom of 10 strains can affect plant protection by SynComs.

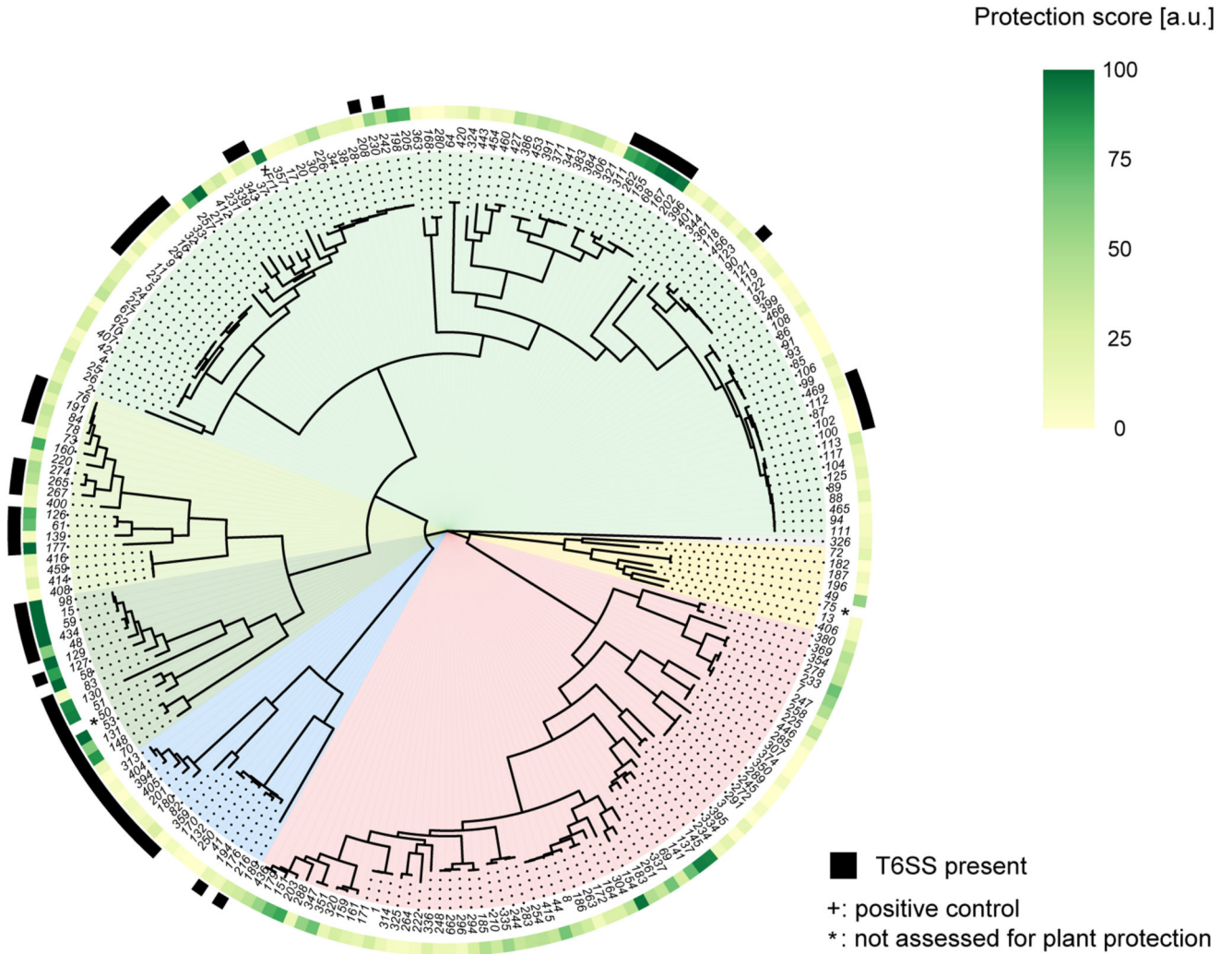
Plants were inoculated with random SynComs of 10 strains, drop-out communities thereof or individual strains and infected with lux-tagged *Pseudomonas syringae* DC3000 (Pst). **a**) Distribution of disease scores at 13 days post infection (dpi) on a scale of 1 (healthy) to 5 (dead). **b**) Luminescence as proxy of pathogen colonization at 6 dpi. Boxplots depict the median and interquartile range with whiskers extending to maximum 1.5x the interquartile range. P-values for indicated comparisons are shown (two-sided Welch's t-test, $n = 21$ -24 plants per condition). Exact number of replicates are provided in Supplementary Table 6. **c**) Colonization by the individual SynComs on non-infected plants at 12 days post inoculation. Shown are the mean and individual data points of 3 replicates consisting of 2 plants each.



Extended Data Figure 6. SynComs of three strains can improve protection phenotypes relative to individual strains.

Plants were inoculated with SynComs of three strains (M3.1, M3.2 and M3.3; comprised of non-protective and intermediate protective strains) or the strains individually and infected with lux-tagged *Pseudomonas syringae* DC3000 (Pst). **a**) Distribution of disease scores on

a scale of 1 (healthy) to 5 (dead) at 13 days post infection (dpi). **b**) Pathogen luminescence at 6 dpi ($\log_{10}(p/s)$). Boxplots depict the median and interquartile range with whiskers extending to maximum 1.5x the interquartile range. Letters indicate statistical significance within each SynCom (one-way ANOVA with Tukey's post-hoc test, $n = 16-24$). Exact p-values and number of replicates are provided in Supplementary Table 8.



Extended Data Figure 7. T6SS gene cluster presence in At-LSPHERE strains and *Spingomonas melonis* Fr1.

The outer rings reflect mean protection scores against Pst on Col-0 plants and the presence of predicted T6SS gene clusters, respectively. a.u.: arbitrary units.

Supplementary Material

Refer to Web version on PubMed Central for supplementary material.

Acknowledgements

We would like to thank Dr. Miriam Bortfeld-Miller for technical assistance and Dr. Asaf Levy for helpful discussions. *A. thaliana bak1/bkk1* was kindly provided by Dr. Cyril Zipfel (University of Zurich, Switzerland). The study was supported by an ERC Advanced Research Grant (PhyMo - 668991 to JAV), ETH Zurich, a grant from the German Research Foundation (DECRyPT, no. SPP2125 to JAV) and the NCCR Microbiomes (to JAV), funded by the Swiss National Science Foundation.

Data availability statement

Source data are provided with this paper. Sequencing data for this study have been deposited in the European Nucleotide Archive (ENA) under accession PRJEB47672. Other genome data are available from NCBI under accessions PRJNA297956, PRJNA471493 and PRJNA84361. The EggNOG-Database is available from <http://eggnog45.embl.de/#/app/home>. *Rhizobium* genomes used for comparative genomics are available from <https://img.jgi.doe.gov/m> under IMG Genome IDs 2643221743, 2643221780, 2643221832, 2643221860, 2643221889, 2643221891, 2643221896, 2643221905, 2643221915, 2643221931, 2643221933-36.

Code availability statement

The scripts used for sequencing data processing, genome assembly and data analysis are available at https://gitlab.ethz.ch/chvogel1/vogel_natmicro_2021/.

References

1. Müller DB, Vogel C, Bai Y, Vorholt JA. The plant microbiota: systems-level insights and perspectives. *Annu Rev Genet.* 2016; 50: 211–234. [PubMed: 27648643]
2. Udvardi M, Poole PS. Transport and metabolism in legume-rhizobia symbioses. *Annu Rev Plant Biol.* 2013; 64: 781–805. [PubMed: 23451778]
3. Parniske M. Arbuscular mycorrhiza: the mother of plant root endosymbioses. *Nat Rev Microbiol.* 2008; 6: 763–775. [PubMed: 18794914]
4. Bulgarelli D, Schlaeppi K, Spaepen S, Ver Loren van Themaat E, Schulze-Lefert P. Structure and functions of the bacterial microbiota of plants. *Annu Rev Plant Biol.* 2013; 64: 807–838. [PubMed: 23373698]
5. Wagner MR, et al. Natural soil microbes alter flowering phenology and the intensity of selection on flowering time in a wild *Arabidopsis* relative. *Ecol Lett.* 2014; 17: 717–726. [PubMed: 24698177]
6. Glick BR. Bacteria with ACC deaminase can promote plant growth and help to feed the world. *Microbiol Res.* 2014; 169: 30–39. [PubMed: 24095256]
7. Ritpitakphong U, et al. The microbiome of the leaf surface of *Arabidopsis* protects against a fungal pathogen. *New Phytol.* 2016; 210: 1033–1043. [PubMed: 26725246]
8. Compant S, Duffy B, Nowak J, Clement C, Barka EA. Use of plant growth-promoting bacteria for biocontrol of plant diseases: principles, mechanisms of action, and future prospects. *Appl Environ Microbiol.* 2005; 71: 4951–4959. [PubMed: 16151072]
9. Santhanam R, et al. Native root-associated bacteria rescue a plant from a sudden-wilt disease that emerged during continuous cropping. *Proc Natl Acad Sci USA.* 2015; 112: E5013–5020. [PubMed: 26305938]
10. Carrión VJ, et al. Pathogen-induced activation of disease-suppressive functions in the endophytic root microbiome. *Science.* 2019; 366: 606–612. [PubMed: 31672892]
11. Toju H, et al. Core microbiomes for sustainable agroecosystems. *Nat Plants.* 2018; 4: 247–257. [PubMed: 29725101]

12. Vorholt JA, Vogel C, Carlström CI, Müller DB. Establishing causality: opportunities of synthetic communities for plant microbiome research. *Cell Host Microbe*. 2017; 22: 142–155. [PubMed: 28799900]
13. Busby PE, et al. Research priorities for harnessing plant microbiomes in sustainable agriculture. *PLoS Biol*. 2017; 15 e2001793 [PubMed: 28350798]
14. Berg G. Plant-microbe interactions promoting plant growth and health: perspectives for controlled use of microorganisms in agriculture. *Appl Microbiol Biotechnol*. 2009; 84: 11–18. [PubMed: 19568745]
15. Cook, RJ. *Encyclopedia of Agriculture and Food Systems*. Van Alfen, NK, editor. Vol. 4. Academic Press; 2014. 441–455.
16. Weller DM, Raaijmakers JM, Gardener BB, Thomashow LS. Microbial populations responsible for specific soil suppressiveness to plant pathogens. *Annu Rev Phytopathol*. 2002; 40: 309–348. [PubMed: 12147763]
17. Latz E, Eisenhauer N, Rall BC, Scheu S, Jousset A. Unravelling linkages between plant community composition and the pathogen-suppressive potential of soils. *Sci Rep*. 2016; 6 23584 [PubMed: 27021053]
18. Finkel OM, Castrillo G, Herrera Paredes S, Salas González I, Dangl JL. Understanding and exploiting plant beneficial microbes. *Curr Opin Plant Biol*. 2017; 38: 155–163. [PubMed: 28622659]
19. Jacobsen, BJ. CAB International. Bailey, MJ, Lilley, AK, Timms-Wilson, TM, Spencer-Phillips, PTN, editors. Wallingford; 2006. 133–147.
20. Barbey C, et al. In planta biocontrol of *Pectobacterium atrosepticum* by *Rhodococcus erythropolis* involves silencing of pathogen communication by the rhodococcal gamma-lactone catabolic pathway. *PLoS ONE*. 2013; 8
21. Pieterse CM, et al. Induced systemic resistance by beneficial microbes. *Annu Rev Phytopathol*. 2014; 52: 347–375. [PubMed: 24906124]
22. Dangl JL, Horvath DM, Staskawicz BJ. Pivoting the plant immune system from dissection to deployment. *Science*. 2013; 341: 746–751. [PubMed: 23950531]
23. Bodenhausen N, Bortfeld-Miller M, Ackermann M, Vorholt JA. A synthetic community approach reveals plant genotypes affecting the phyllosphere microbiota. *PLoS Genet*. 2014; 10 e1004283 [PubMed: 24743269]
24. Lebeis SL, et al. PLANT MICROBIOME. Salicylic acid modulates colonization of the root microbiome by specific bacterial taxa. *Science*. 2015; 349: 860–864. [PubMed: 26184915]
25. Pfeilmeier S, et al. The plant NADPH oxidase RBOHD is required for microbiota homeostasis in leaves. *Nat Microbiol*. 2021; 6: 852–864. [PubMed: 34194036]
26. Chen T, et al. A plant genetic network for preventing dysbiosis in the phyllosphere. *Nature*. 2020; 580: 653–657. [PubMed: 32350464]
27. Innerebner G, Knief C, Vorholt JA. Protection of *Arabidopsis thaliana* against leaf-pathogenic *Pseudomonas syringae* by *Sphingomonas* strains in a controlled model system. *Appl Environ Microbiol*. 2011; 77: 3202–3210. [PubMed: 21421777]
28. Vogel C, Bodenhausen N, Gruijssem W, Vorholt JA. The *Arabidopsis* leaf transcriptome reveals distinct but also overlapping responses to colonization by phyllosphere commensals and pathogen infection with impact on plant health. *New Phytol*. 2016; 212: 192–207. [PubMed: 27306148]
29. Karasov TL, et al. *Arabidopsis thaliana* and *Pseudomonas* pathogens exhibit stable associations over evolutionary timescales. *Cell Host Microbe*. 2018; 24: 168–179. e164 [PubMed: 30001519]
30. Bai Y, et al. Functional overlap of the *Arabidopsis* leaf and root microbiota. *Nature*. 2015; 528: 364–369. [PubMed: 26633631]
31. Vogel C, Innerebner G, Zingg J, Guder J, Vorholt JA. Forward genetic *in planta* screen for identification of plant-protective traits of *Sphingomonas* sp. strain Fr1 against *Pseudomonas syringae* DC3000. *Appl Environ Microbiol*. 2012; 78: 5529–5535. [PubMed: 22660707]
32. Helfrich EJN, et al. Bipartite interactions, antibiotic production and biosynthetic potential of the *Arabidopsis* leaf microbiome. *Nat Microbiol*. 2018; 3: 909–919. [PubMed: 30038309]

33. Cenicerros A, Dijkhuizen L, Petrusma M, Medema MH. Genome-based exploration of the specialized metabolic capacities of the genus *Rhodococcus*. *BMC Genomics*. 2017; 18: 593. [PubMed: 28793878]
34. Ma XY, Xu GY, He P, Shan LB. SERKing coreceptors for receptors. *Trends Plant Sci*. 2016; 21: 1017–1033. [PubMed: 27660030]
35. Ma LS, Hachani A, Lin JS, Filloux A, Lai EM. *Agrobacterium tumefaciens* deploys a superfamily of type VI secretion DNase effectors as weapons for interbacterial competition in planta. *Cell Host Microbe*. 2014; 16: 94–104. [PubMed: 24981331]
36. Bernal P, Allsopp LP, Filloux A, Llamas MA. The *Pseudomonas putida* T6SS is a plant warden against phytopathogens. *ISME J*. 2017; 11: 972–987. [PubMed: 28045455]
37. Decoin V, et al. A *Pseudomonas fluorescens* type 6 secretion system is related to mucoidy, motility and bacterial competition. *BMC Microbiol*. 2015; 15: 72. [PubMed: 25886496]
38. Goberna M, Verdu M. Predicting microbial traits with phylogenies. *ISME J*. 2016; 10: 959–967. [PubMed: 26371406]
39. Melnyk RA, Hossain SS, Haney CH. Convergent gain and loss of genomic islands drive lifestyle changes in plant-associated *Pseudomonas*. *ISME J*. 2019; 13: 1575–1588. [PubMed: 30787396]
40. Haney CH, Samuel BS, Bush J, Ausubel FM. Associations with rhizosphere bacteria can confer an adaptive advantage to plants. *Nat Plants*. 2015; 1: 15051 [PubMed: 27019743]
41. Savory EA, et al. Evolutionary transitions between beneficial and phytopathogenic *Rhodococcus* challenge disease management. *Elife*. 2017; 6
42. Haas D, Défago G. Biological control of soil-borne pathogens by fluorescent pseudomonads. *Nat Rev Microbiol*. 2005; 3: 307–319. [PubMed: 15759041]
43. Raaijmakers JM, et al. Dose-response relationships in biological-control of Fusarium wilt of radish by *Pseudomonas* spp. *Phytopathol*. 1995; 85: 1075–1081.
44. Kwak MJ, et al. Rhizosphere microbiome structure alters to enable wilt resistance in tomato. *Nat Biotechnol*. 2018; 36: 1100–1109.
45. Berg M, Koskella B. Nutrient- and dose-dependent microbiome-mediated protection against a plant pathogen. *Curr Biol*. 2018; 28: 2487–2492. [PubMed: 30057302]
46. Berendsen RL, et al. Disease-induced assemblage of a plant-beneficial bacterial consortium. *ISME J*. 2018; 12: 1496–1507. [PubMed: 29520025]
47. Rudrappa T, Czymmek KJ, Pare PW, Bais HP. Root-secreted malic acid recruits beneficial soil bacteria. *Plant Physiol*. 2008; 148: 1547–1556. [PubMed: 18820082]
48. Liu H, Brettell LE, Qiu Z, Singh BK. Microbiome-mediated stress resistance in plants. *Trends Plant Sci*. 2020; 25: 733–743. [PubMed: 32345569]
49. Song Y, et al. Loss of a plant receptor kinase recruits beneficial rhizosphere-associated *Pseudomonas*. *bioRxiv*. 2020.
50. Bartoli C, et al. *In situ* relationships between microbiota and potential pathobiota in *Arabidopsis thaliana*. *ISME J*. 2018; 12: 2024–2038. [PubMed: 29849170]
51. Andrews JH. Biological control in the phyllosphere. *Annu Rev Phytopathol*. 1992; 30: 603–635. [PubMed: 18647102]
52. Raaijmakers JM, Mazzola M. Diversity and natural functions of antibiotics produced by beneficial and plant pathogenic bacteria. *Annu Rev Phytopathol*. 2012; 50: 403–424. [PubMed: 22681451]
53. Lindow SE, Brandl MT. Microbiology of the phyllosphere. *Appl Environ Microbiol*. 2003; 69: 1875–1883. [PubMed: 12676659]
54. Monier JM, Lindow SE. Frequency, size, and localization of bacterial aggregates on bean leaf surfaces. *Appl Environ Microbiol*. 2004; 70: 346–355. [PubMed: 14711662]
55. Remus-Emsermann MNP, et al. Spatial distribution analyses of natural phyllosphere-colonizing bacteria on *Arabidopsis thaliana* revealed by fluorescence in situ hybridization. *Environ Microbiol*. 2014; 16: 2329–2340. [PubMed: 24725362]
56. Wei Z, et al. Trophic network architecture of root-associated bacterial communities determines pathogen invasion and plant health. *Nat Commun*. 2015; 6: 8413 [PubMed: 26400552]
57. An SQ, et al. Mechanistic insights into host adaptation, virulence and epidemiology of the phytopathogen *Xanthomonas*. *FEMS Microbiol Rev*. 2020; 44: 1–32. [PubMed: 31578554]

58. Chaston JM, Newell PD, Douglas AE. Metagenome-wide association of microbial determinants of host phenotype in *Drosophila melanogaster*. *Mbio*. 2014; 5 e01631-01614 [PubMed: 25271286]
59. MacDonald NJ, Beiko RG. Efficient learning of microbial genotype-phenotype association rules. *Bioinformatics*. 2010; 26: 1834–1840. [PubMed: 20529891]
60. Levy A, et al. Genomic features of bacterial adaptation to plants. *Nat Genet*. 2018; 50: 138–150.
61. Ryu CM. Against friend and foe: type 6 effectors in plant-associated bacteria. *J Microbiol*. 2015; 53: 201–208. [PubMed: 25732741]
62. Bernal P, Llamas MA, Filloux A. Type VI secretion systems in plant-associated bacteria. *Environ Microbiol*. 2018; 20: 1–15. [PubMed: 29027348]
63. Decoin V, et al. A type VI secretion system is involved in *Pseudomonas fluorescens* bacterial competition. *PLoS ONE*. 2014; 9 e89411 [PubMed: 24551247]
64. Mosquito S, et al. In planta colonization and role of T6SS in two rice *Kosakonia* endophytes. *Mol Plant Microbe Interact*. 2020; 33: 349–363. [PubMed: 31609645]
65. Vlot AC, et al. Systemic propagation of immunity in plants. *New Phytol*. 2021; 229: 1234–1250. [PubMed: 32978988]
66. Roux M, et al. The Arabidopsis leucine-rich repeat receptor-like kinases BAK1/SERK3 and BKK1/SERK4 are required for innate immunity to hemibiotrophic and biotrophic pathogens. *Plant Cell*. 2011; 23: 2440–2455. [PubMed: 21693696]
67. Fan J, Crooks C, Lamb C. High-throughput quantitative luminescence assay of the growth in planta of *Pseudomonas syringae* chromosomally tagged with *Photobacterium luminescens luxCDABE*. *Plant J*. 2008; 53: 393–399. [PubMed: 17971037]
68. Wu YW. ezTree: an automated pipeline for identifying phylogenetic marker genes and inferring evolutionary relationships among uncultivated prokaryotic draft genomes. *BMC Genomics*. 2018; 19: 921. [PubMed: 29363425]
69. Bushnell B. BBMap: short read aligner, and other bioinformatic tools. Available from: <https://sourceforge.net/projects/bbmap/>.
70. Andrews S. FastQC: A quality control tool for high throughput sequence data. Babraham Institute. 2010. Available online at: <https://www.bioinformatics.babraham.ac.uk/projects/fastqc/>.
71. Bankevich A, et al. SPAdes: a new genome assembly algorithm and its applications to single-cell sequencing. *J Comput Biol*. 2012; 19: 455–477. [PubMed: 22506599]
72. Seemann T. Prokka: rapid prokaryotic genome annotation. *Bioinformatics*. 2014; 30: 2068–2069. [PubMed: 24642063]
73. Jain C, Rodriguez RL, Phillippy AM, Konstantinidis KT, Aluru S. High throughput ANI analysis of 90K prokaryotic genomes reveals clear species boundaries. *Nat Commun*. 2018; 9 5114 [PubMed: 30504855]
74. Revell LJ. phytools: an R package for phylogenetic comparative biology (and other things). *Methods Ecol Evol*. 2012; 3: 217–223.
75. Jombart T, Balloux F, Dray S. adephylo: new tools for investigating the phylogenetic signal in biological traits. *Bioinformatics*. 2010; 26: 1907–1909. [PubMed: 20525823]
76. Chen IA, et al. IMG/M v.5.0: an integrated data management and comparative analysis system for microbial genomes and microbiomes. *Nucl Acids Res*. 2019; 47: D666–D677. [PubMed: 30289528]
77. Mukherjee S, et al. Genomes OnLine database (GOLD) v.7: updates and new features. *Nucl Acids Res*. 2019; 47: D649–D659. [PubMed: 30357420]
78. Huerta-Cepas J, et al. Fast genome-wide functional annotation through orthology assignment by eggNOG-mapper. *Mol Biol Evol*. 2017; 34: 2115–2122. [PubMed: 28460117]
79. Huerta-Cepas J, et al. eggNOG 4.5: a hierarchical orthology framework with improved functional annotations for eukaryotic, prokaryotic and viral sequences. *Nucl Acids Res*. 2016; 44: D286–293. [PubMed: 26582926]
80. Abby SS, et al. Identification of protein secretion systems in bacterial genomes. *Sci Rep*. 2016; 6 23080 [PubMed: 26979785]

81. Boyer F, Fichant G, Berthod J, Vandenbrouck Y, Attree I. Dissecting the bacterial type VI secretion system by a genome wide *in silico* analysis: what can be learned from available microbial genomic resources? *BMC Genomics*. 2009; 10: 104. [PubMed: 19284603]
82. Lin JS, Ma LS, Lai EM. Systematic dissection of the agrobacterium type VI secretion system reveals machinery and secreted components for subcomplex formation. *PLoS One*. 2013; 8 e67647 [PubMed: 23861778]
83. Ledermann R, Strebel S, Kampik C, Fischer HM. Versatile vectors for efficient mutagenesis of *Bradyrhizobium diazoefficiens* and other Alphaproteobacteria. *Appl Environ Microbiol*. 2016; 82: 2791–2799. [PubMed: 26921431]
84. Wu CF, et al. Plant-pathogenic *Agrobacterium tumefaciens* strains have diverse type VI effector-immunity pairs and vary in in-planta competitiveness. *Mol Plant Microbe Interact*. 2019; 32: 961–971. [PubMed: 30830835]
85. Kassambra A. rstatix: Pipe-friendly framework for basic statistical tests. R package version 0.6.0. 2020. <https://CRAN.R-project.org/package=rstatix>
86. Pinheiro J, DebRoy S, Sarkar D, Team RC. nlme: Linear and Nonlinear Mixed Effects Models. R package version 3.1-144. 2020. URL: <https://CRAN.R-project.org/package>
87. Lenth, R. emmeans: Estimated marginal means, aka least-squares means. 2020.
88. Paradis E, Schliep K. ape 5.0: an environment for modern phylogenetics and evolutionary analyses in R. *Bioinformatics*. 2019; 35: 526–528. [PubMed: 30016406]
89. Gu ZG, Gu L, Eils R, Schlesner M, Brors B. circlize implements and enhances circular visualization in R. *Bioinformatics*. 2014; 30: 2811–2812. [PubMed: 24930139]
90. Wickham H, et al. Welcome to the Tidyverse. *J Open Source Softw*. 2019; 4 1686

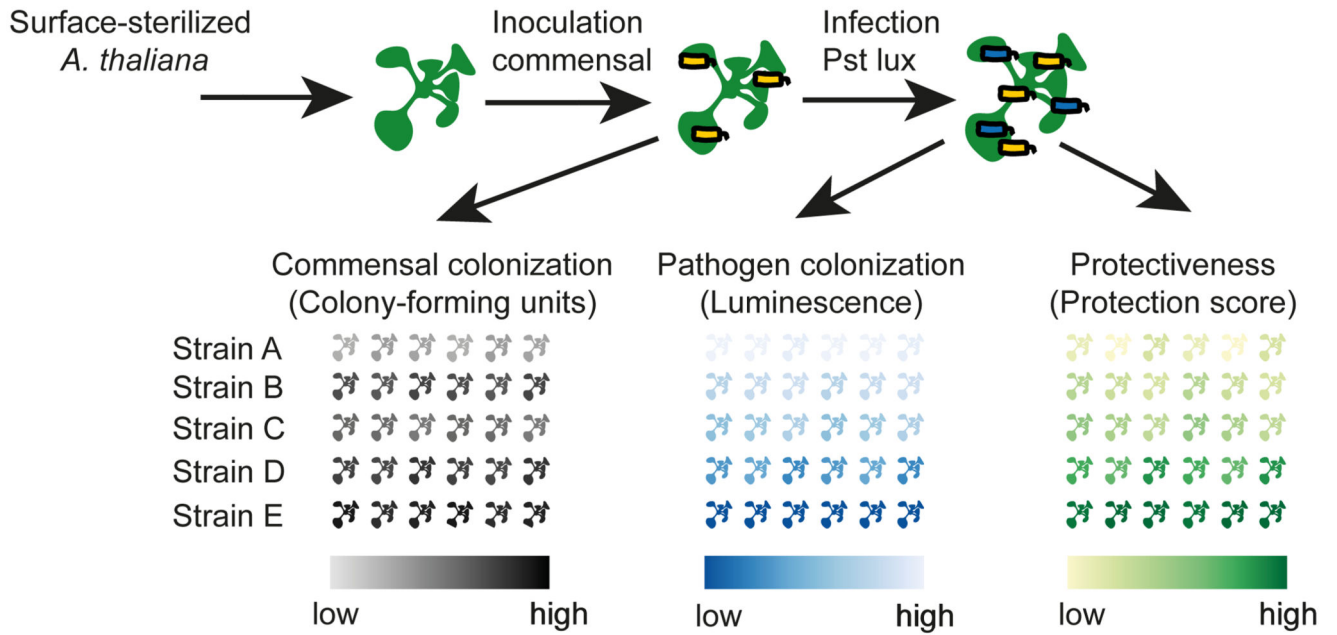


Fig. 1. Overview of experimental screening system.

A. thaliana seeds were surface sterilized and grown in 24-well plates on agar. At 10 days, leaves were inoculated with a suspension of a commensal strain to be tested for protection ability and the strain left to colonize the plants. At 15 days, plants were challenged with a *luxCDABE*-tagged *Pseudomonas syringae* DC3000 (Pst). Pathogen infection or lack thereof was scored in two ways. Luminescence quantification at 6 days post infection was used as a proxy for pathogen colonization. Disease scoring based on symptoms was used to calculate the protection score relative to the disease observed in control plants. Furthermore, we used uninfected plants to determine phyllosphere colonization by the commensal strains by counting colony-forming units after a wash protocol.

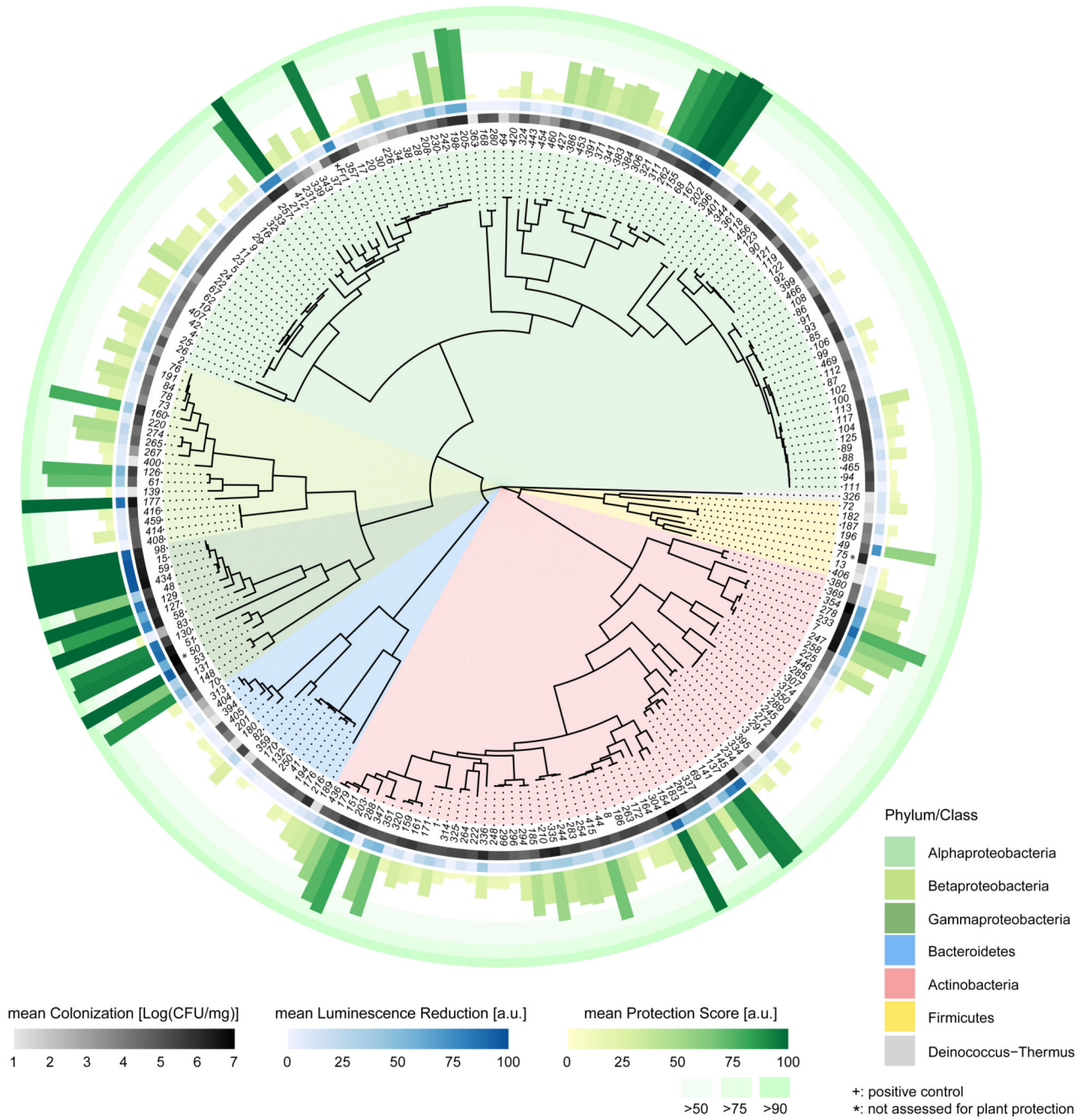


Fig. 2. Overview of plant protection in the At-LSPHERE.
 Plant protection by individual strains against a *luxCDABE*-tagged *Pseudomonas syringae* DC3000. Phylogenetic tree of bacterial strains of the At-LSPHERE and the positive control *S. melonis* Fr1 with the background colors corresponding to phyla and class. The inner ring (grey scale) depicts the strain colonization as log₁₀-transformed colony-forming units (CFU) per gram plant fresh weight at 9 days after inoculation. The second ring (blue scale) corresponds to luminescence reduction and hence reduction of pathogen colonization at 6 days post infection. The outer ring (green scale) reflects the protectiveness (i.e. protection

against disease) with the height and color of the barcode both corresponding to the mean protection score. The concentric rings in the background indicate a mean protection score of 50-75, 75-90 and 90-100, respectively. Asterisks: strain was not assessed for plant protection (see Methods). The phylogenetic tree is based on whole genome sequences.

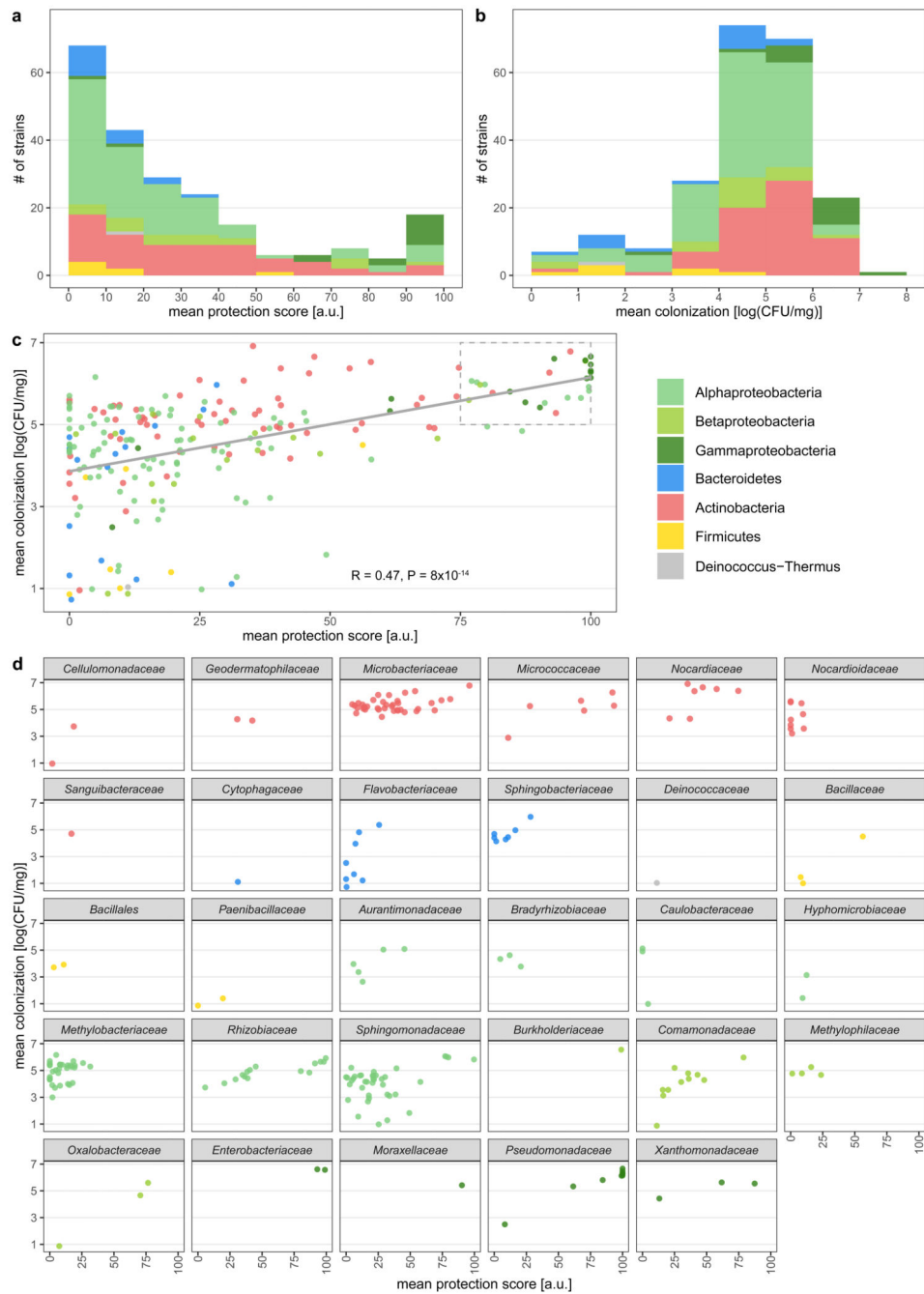


Fig. 3. Protective strains of the *At*-LSPHERE colonize the phyllosphere at high density. **a**, Histogram of mean protection score ($n = 222$ strains) and **b**, of mean colonization ($n = 224$ strains) for the *At*-LSPHERE collection. **c**, Correlation of mean colonization (log₁₀-transformed) and mean protection score (Pearson's $R = 0.47$, $t = 7.97$, $df = 223$, $P = 8 \times 10^{-14}$). The linear regression line is indicated. The dashed box highlights mean colonization above 10^5 CFU/mg and mean protection score >75. **d**, Mean colonization plotted against mean protection score for each family separately. Colors throughout the figure correspond to phyla and class. Exact numbers of independent experiments and

biological replicates within experiment for each strain are provided in Supplementary Tables 1 and 2, respectively.

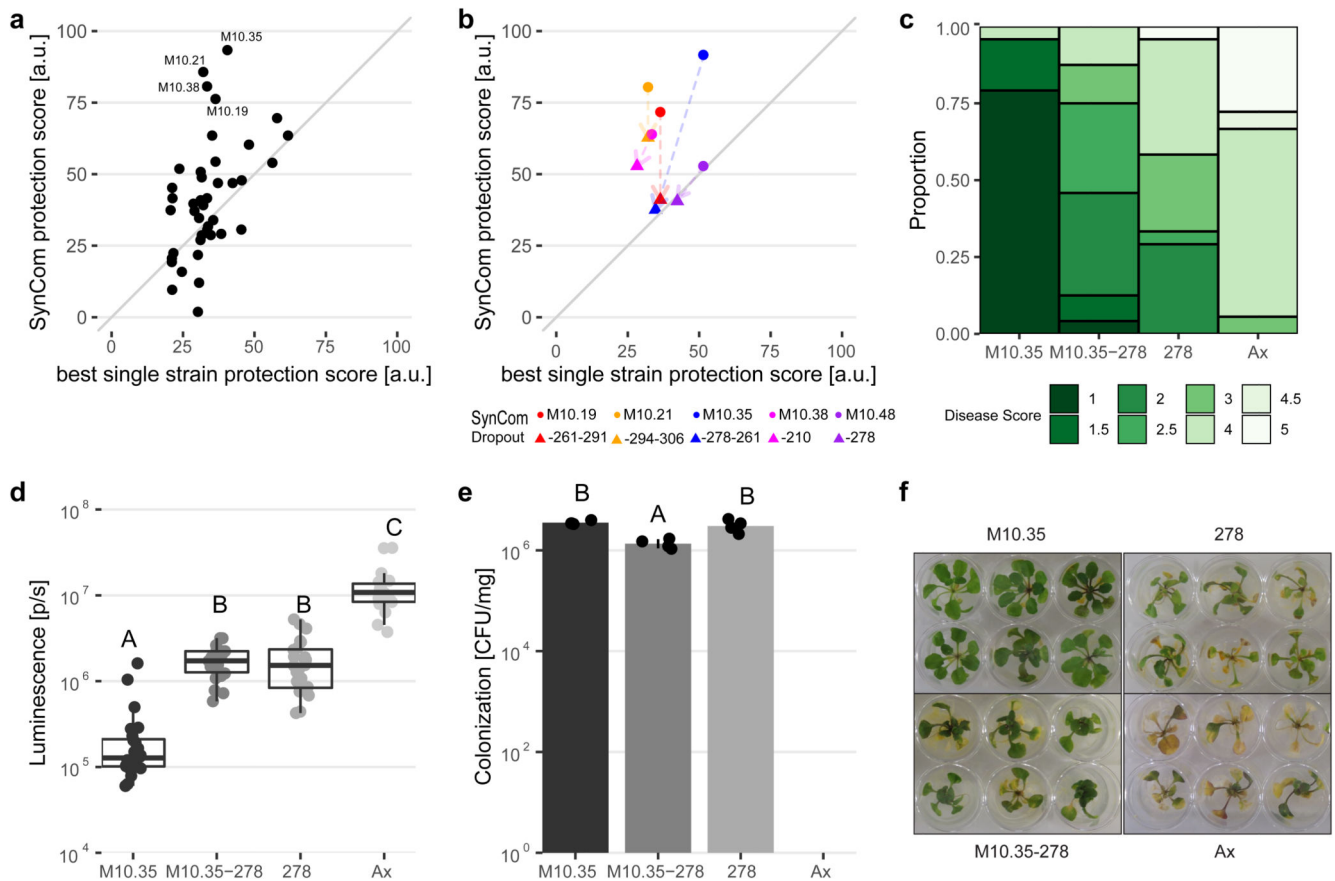


Fig. 4. SynCom experiments reveal community-specific gain of protection.

Random SynComs of 10 non-protective strains were inoculated onto *A. thaliana* plants 5 days prior to infection with lux-tagged *Pseudomonas syringae* (Pst) and disease symptoms scored at 13 days post infection (dpi). **a**, Protection score of random SynComs plotted against the mean protection score of the best single strain within the mix. Mixes for which dropouts were tested in a separate experiment are labelled. **b**, Dropout of indicated strains from 5 random SynComs and the effect on the protection by the respective SynCom. Arrows indicate the change in protection from full to drop-out SynCom. **c-f**, Plants were inoculated with random SynCom M10.35, SynCom M10.35 without Leaf278 (M10.35-278), Leaf278 alone or buffer (Ax). Five days post inoculation plants were challenged with Pst (**c,d,f**). **d**, Boxplots of pathogen luminescence at 6 dpi (n = 18-24 plants per condition). Boxplots center line, median; box limits, upper and lower quartiles; whiskers, 1.5x interquartile range; points, outliers. **c**, Distribution of disease scores on a scale from 1 (healthy) to 5 (dead) (**c**) with representative images at 13 dpi (**f**). Colonization of non-infected plants at 12 days post inoculation (**e**). Shown are median and individual data points of 4 replicates representing a pool of two plants each. Letters indicate significant differences based on one-way ANOVA and Tukey's post-hoc test. Exact p-values and number of replicates are provided in Supplementary Table 7.

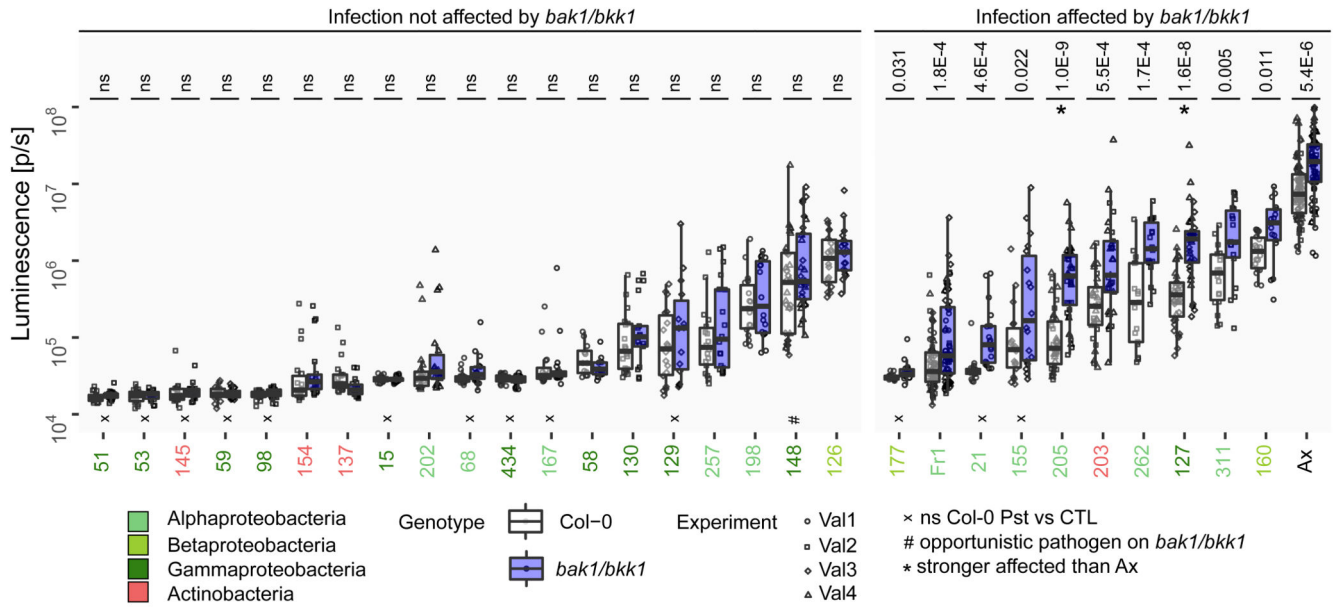


Fig. 5. Plant protection in the *bak1/bkk1* plant background is strongly reduced in a subset of strains based on luminescence analysis.

Shown is the luminescence at 6 days post infection with the *lux*-tagged *Pseudomonas syringae* (Pst) for *bak1/bkk1* and Col-0 plants inoculated with a commensal or mock control (Ax) prior to infection. Boxplots depict the median and interquartile range with whiskers extending up to 1.5x the interquartile range. Strains are grouped by the effect the *bak1/bkk1* genotype had on infection based on luminescence. *P*-values for the comparison of *bak1/bkk1* and Col-0 infected plants are indicated (one-sided Welch's test, *p*-value adjusted using Benjamini-Hochberg's method, ns: *p*-value >0.05). Asterisk: effect of *bak1/bkk1* genotype on infection is significantly higher than in the axenic control (see methods). x: luminescence in Col-0 not significantly higher with infection (i.e. one-sided Welch's test, *p*-value adjusted using Benjamini-Hochberg's method). Number sign: opportunistic pathogen on *bak1/bkk1*. Shown are data for protective strains (mean protection score in Col-0 plants >75) and controls (Fr1 and Ax). For others, see Supplementary Figure 4. Data are from 1-4 independent experiments with 16-18 plant replicates per experiment. Exact *p*-values and number of replicates within experiment are provided in Supplementary Tables 9 and 10, respectively.

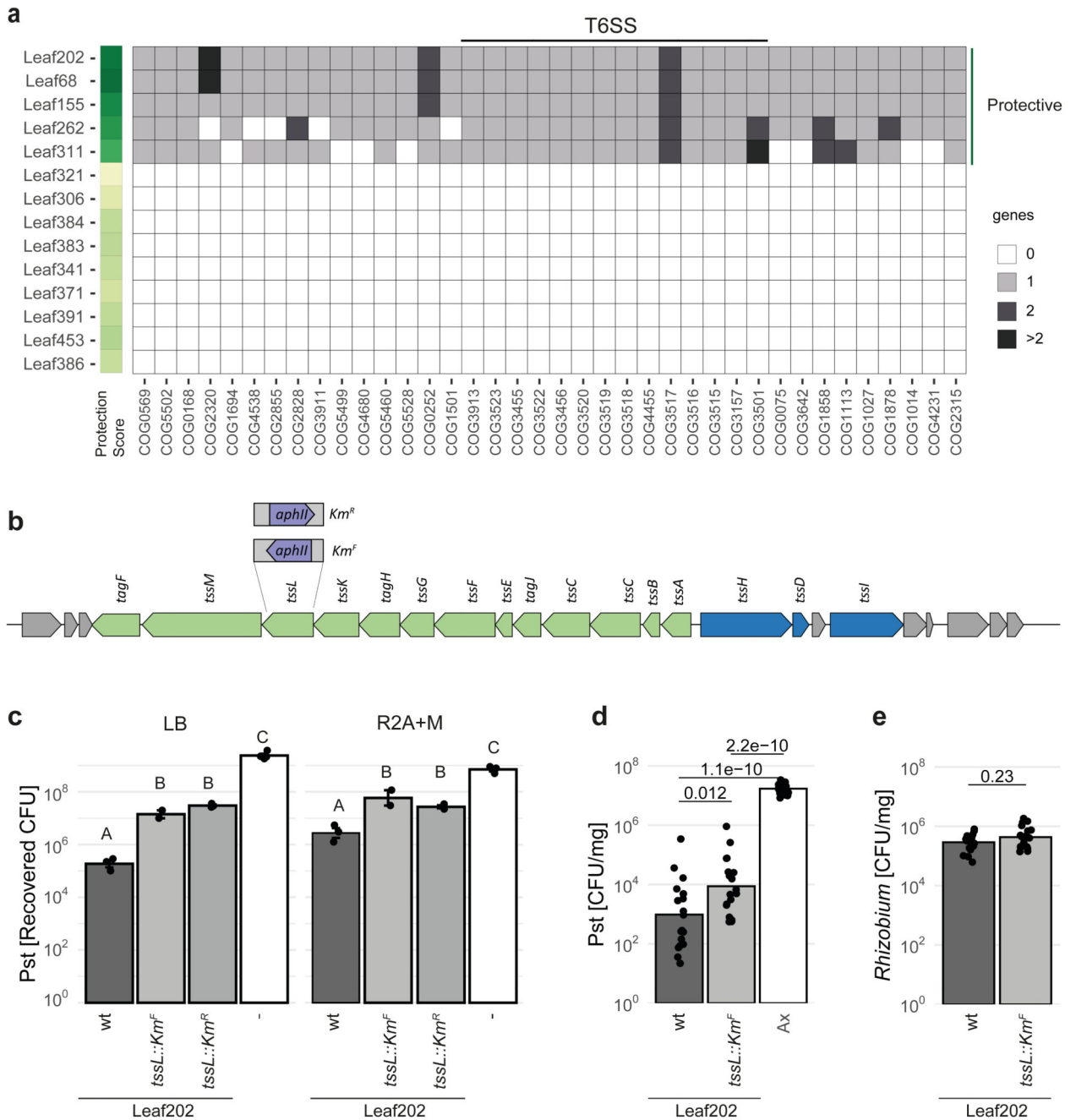


Fig. 6. The T6SS is associated with plant protection in *Rhizobium* spp. in the *At*-LSPHERE.
a, Heatmap of cluster of orthologous genes (COGs) present in protective but not non-protective *Rhizobium* spp. with the COGs associated with the Type 6 secretion system (T6SS) marked. **b**, T6SS gene cluster of *Rhizobium* Leaf202 with the gene-replacement for the *tssL* mutants indicated. **c**, *In vitro* inhibition of Pst by Leaf202 and the *tssL::aphII* mutants (*tssL::Km^R* and *tssL::Km^F* with opposing directions of *aphII* cassette) on LB-Lennox (LB) and R2A supplemented with methanol (R2A+M). Shown are the mean and standard error with individual data points ($n = 3$ independent cultures except for *tssL::Km^F*

n = 2; media controls n = 4 for LB, n = 3 for R2A+M). Letters indicate significant differences (one-way ANOVA followed by Tukey's post-hoc test). **d**, *In planta* inhibition of Pst colonization at 7 days post infection by Leaf202 and its *tssL::Km^F* mutant (n = 19, 18, 18 for wt, *tssL::Km^F* and Ax, respectively). **e**, *In planta* colonization by Leaf202 and its *tssL::Km^F* mutant at 12 days post inoculation (n = 19 and 18 for wt and *tssL::Km^F*, respectively). Shown are the mean and individual data points (**d-e**). *P*-values of two-sided Welch's t-tests are indicated. The plant experiment was performed twice with similar results.